JOINT EUROPEAN TORUS

JET–P(91)11

K.J. Dietz, P. Chappuis, H Horiike, G.L. Jackson, M. Ulrickson
and JET Team

Experience with High Heat Flux Components in Large Tokamaks

"This document contains JET information in a form not yet suitable for publication. The report has been prepared primarily for discussion and information within the JET Project and the Associations. It must not be quoted in publications or in Abstract Journals. External distribution requires approval from the Publications Officer, JET Joint Undertaking, Abingdon, Oxon, OX14 3EA, UK".

"Enquiries about Copyright and reproduction should be addressed to the Publications Officer, EFDA, Culham Science Centre, Abingdon, Oxon, OX14 3DB, UK."

The contents of this preprint and all other JET EFDA Preprints and Conference Papers are available to view online free at www.iop.org/Jet. This site has full search facilities and e-mail alert options. The diagrams contained within the PDFs on this site are hyperlinked from the year 1996 onwards.

Experience with High Heat Flux Components in Large Tokamaks

K.J. Dietz, P. Chappuis[1], H Horiike[2], G.L. Jackson[3], M. Ulrickson[4]
and JET Team*

JET-Joint Undertaking, Culham Science Centre, OX14 3DB, Abingdon, UK

[1]CEN Cadarache, Saint Paullez Durance, CEDEX, France.
[2]Japan Atomic Energy Research Institute, Naka Fusion Research Establlishment, Mukoh-yama, Naka-machi, Naka-gun, lbaraki 311-02, Japan.
[3]General Atomics, San Diego, CA, USA.
[4]Princeton University Plasma Physics Laboratory, Princeton, NJ, USA.
** See Appendix 1*

Preprint of Paper presented at
ISFNT 2, Karlsruhe

Experience with High Heat Flux Components in Large Tokamaks

K. J. Dietz[1], P. Chappuis[2], H. Horiike[3], G. L. Jackson[4], M. Ulrickson[5]

[1]JET Joint Undertaking, Abingdon, OX 14 3EA, United Kingdom, [2]CEN Cadarache, 13108 Saint Paul lez Durance, CEDEX, France, [3]Japan Atomic Energy Research Institute, Naka Fusion Research Establishment, Mukoh-yama, Naka-machi, Naka-gun, Ibaraki 311-02, Japan, [4]General Atomics P.O. Box 85608, San Diego, CA 92186, USA, [5]Princeton University Plasma Physics Laboratory P.O. Box 451, Princeton, NJ 08544, USA

ABSTRACT

The large present day tokamaks i.e. JET, TFTR, JT-60, DIII-D ,and Tore Supra are machines capable of sustaining plasma currents of several million amperes . Pulse durations range from a few seconds up to a minute. These large machines have been in operation for several years and there exists wide experience with materials for plasma facing components. Bare and coated metals, bare and coated graphites and beryllium were used for walls, limiters and divertors. High heat flux components are mainly radiation cooled, but stationary cooling for long pulse duration is also employed. This paper summarizes the experience gained in the large machines with respect to material selection, component design, problem areas, and plasma performance.

1. INTRODUCTION

The large tokamaks, JET, TFTR, JT-60, DIII-D, and Tore Supra, are capable to sustain plasma currents of several million amperes (MA), up to seven for JET. The pulse durations last from a few seconds up to a minute for Tore Supra and JET albeit at reduced plasma current and for JET also at reduced toroidal field.

TFTR and JET are designed to employ a deuterium tritium mixture as working gas to study the plasma behaviour with alpha particle heating in order to allow predictions for burning tokamaks. The total amount of D-T neutrons produced will, however, be in both machines only of the order of 10^{22} to 10^{23}. For all present day large machines material deterioration under neutron bombardment is not expected and therefore not taken into account for the material selection. Consequently high thermal conductivity graphite can be selected as plasma facing material for high heat flux (HHF) components in present day devices.

Tritium retention in wall materials has already to be considered for TFTR and JET. In both cases it could be shown that there do not exist major problems, because of their comparatively small size, the limited tritium operation scenario and the possibility to deplete the tritium wall inventory by conditioning discharges. For the next generation of machines, however, which may employ graphite as wall armour large inventories might be expected especially due to trapping of tritium at neutron

produced damage sites inside the plasma facing materials or in co-deposited layers of tritium and graphite.

Presently all machines, with the exception of Tore Supra, employ cooling techniques for high heat flux components which are of little relevance for the Next Step machines like ITER. Inertia cooling is used in most cases where the energy conducted to limiters or divertor plates is stored in the materials during discharges and is conducted to cooled support structures or radiated to cooler vessel components in the time intervals between discharges. Tore Supra uses for some wall components stationary cooling were the conducted energy is transferred to the cooling water during the discharges so that the surface of the high heat flux components is in thermal equilibrium with the plasma after a few seconds and the surface temperature becomes constant. This type of cooling will be employed for Next Step devices.

The design of components facing the plasma (walls, wall armour, protection of the vacuum vessel, internal structures as for example limiters, divertor dump plates, launchers for plasma heating and current drive etc.) requires the knowledge of a variety of data. The main ones are related to plasma edge parameters, machine configuration and operation modes, abnormal operating conditions, and materials data.

Tokamaks employ limiters and/or divertors in a variety of configurations and the plasma facing components will have to be designed for the respective configuration. Compromises will be required due to access restrictions for installation, the required compatibility with remote maintenance, possible interference with diagnostics, and the need to install sufficiently large surface areas to reduce thermal loads to acceptable levels.

The knowledge of plasma edge parameters is essential for the design of high heat flux components because particle fluxes and energies and their spatial distribution define the power loads, impurity release rates and thus the life time of HHF components. This will become of particular importance for the next generation of machines where plasma burntimes of tens of minutes are envisaged. The data for the plasma edge are normally not well known and show a strong dependence on configurations and global plasma parameters. Accordingly the design has to incorporate adequate safety margins.

The materials data required include, among others, thermomechanical properties, fatigue behaviour, outgassing rates and data on physical and chemical sputtering. In the present day machines, data on radiation damage are of minor importance. Fatigue data are normally not available, especially not for the advanced materials as carbon fibre composite (CFC) graphite. Therefore component tests are mandatory and form an integral part in the development of HHF components. The material selection normally is only one of the facets of a successful design. It is not only required that the components can sustain the conducted power from the plasma without damage, but that on the other hand the plasma properties do not degrade by interaction with the component and the release of wall material. Therefore, as it is for example is the case in JET, wall components can sustain high loads without

damage, but plasmas degrade and become useless already at much lower power due to accumulation of impurities released at hot spots.

Besides graphite, being used extensively in all tokamaks as fine grain graphite and carbon fibre composite, a variety of other materials have so far been employed for plasma facing components. They range from nickel base alloys (JET), titanium carbide (TiC) coatings on molybdenum (JT-60), TiC coating on graphite (TFTR) and boron nitride (DIII-D) to beryllium (JET). The experience obtained in the large machines is summarized in the following paragraphs.

2. OPERATIONAL EXPERIENCE IN JT-60

JT-60 (major radius of 3.03 m and minor radius 0.995 m) could be operated as limiter or divertor machine with Neutral Beam power up to 25 MW. It was found that wall materials consisting of TiC coated metal plates are superior to carbon tiles as far as control of plasma density and impurity content is concerned. Problems using metal plates were related to bursts of metallic impurities in high power heating discharges. Therefore carbon tiles were installed as replacement. The carbon wall showed very high tolerance against heating experiments with powers of up to 25 MW. Following this experience the wall for JT-60 upgrade was designed to utilize carbon fibre composites for the divertor and isotropic graphite for the other regions. The divertor tiles are cooled by the forced circulation of water or nitrogen gas, while the other regions are cooled by conduction to the vessel wall.

JT-60 began its operation with titaniumcarbide (TiC) coated molybdenum as first wall material. The TiC surface was used for two years operation with ohmic, neutral beam and lower hybrid heating (LHH). During this period no deterioration was observed in the coated TiC films, in contrast to findings of TFTR [1] on their coatings. The use of TiC allowed JT-60 to produce clean, low density plasmas. With these plasmas high T_i [2] and confinement experiments in lower hybrid current driven plasmas [3] could be performed. The divertor plasmas showed low radiation losses of only 10% with beam heating and the convective power flow to the divertor plate amounted to 70% [4]. However, the limiter plasmas suffered radiation losses as high as 60% of total input including beam power, hence the beam heating period was limited due to build-up of high-Z impurities resulting from such metals as Ti and Mo. Due to these impurities the plasma current was also limited to values below 2 MA.

In order to avoid the plasma contamination by high-Z materials and to obtain high current discharges in the limiter configuration, the TiC coated Mo plates were replaced with graphite tiles. With this wall the concentration of metals was suppressed and high current limiter discharges became possible with beam heating of up to 25 MW. Values of Z_{eff} are compared in Fig. 1 for high power beam heated discharges as a function of the line averaged electron density [5]. Impurity concentrations are also summarized in Table 1 where TiC coated walls and graphite walls are compared as well as two divertor configurations. The value of Z_{eff} was lowest in the closed divertor plasma with TiC walls and was highest in the open

divertor plasma with the graphite walls. It is noticeable that the oxygen levels do not change much.

Density limits are compared in Fig. 2 for ohmic plasmas with TiC and graphite walls [6]. Because the recycling coefficient for the TiC wall was estimated to be 0.8 to 0.98, the plasma density was highly reproducible with only simple adjustments in the gas puffing rates required. This was also marked for low density discharges where the recycling rate decreases with density. In contrast to these observations the graphite wall exhibited varying recycling rates shot by shot. Because the wall tended to be saturated with gas particles after a sequence of plasma discharges, low density plasmas became more difficult to be produced and were obtained only after special conditioning discharges [6].

The divertor heat flux is given in Fig. 3. It was measured by an infrared camera system. Asymmetry of the heat flux in the inside and outside regions of the divertor was observed, which was reversed with the change of ion ∇B drift direction.

2.1 FIRST WALL DESIGN FOR JT-60 UPGRADE

The first wall design for JT-60U was based on the experience of JT-60. Since high power heating experiments are expected to be a top priority, graphite was choosen to cover the wall: isotropic graphite for the area other than the divertor and carbon fibre composite in the area of the divertor. The vacuum vessel has a double skin made of thin plates of Inconel 625. The first wall armour, in form of tiles, is fastened to the wall near the cooling channels to increase the thermal conduction from the tiles to the coolant gas. The double walled vessel is mechanically strong against disruption forces, but not very well suited for heat flow across the wall due to the low thermal conductivity between the two skins. Therefore the divertor plate was provided with cooling channels so as to protect the vessel wall from high heat fluxes emanating from the divertor armour. The armour is fitted to the cooled base plate by a backing plate. The design is shown in Fig. 4. The divertor plate has a simple structure but the cooling tubes between the plates are much more complicated because a fraction of the eddy currents, induced in the vessel skin by the disruptive plasma motion, circulates in the tubes. Therefore the tube has many U bends which are carefully attached to the vessel so as to minimize the amount of eddy current circulating in the tube. The divertor plates are also carefully aligned so that the height difference between neighbouring plates is kept below 0.5 mm. The distance between the vacuum vessel and the armour was kept below 6 to 8 cm for the divertor and to 4 to 5 cm for the other areas. These distances were minimized in order to maximize the plasma cross-section which then enables JT-60U to sustain discharges with plasma currents above 6 MA.

The maximum heat flux to the divertor was estimated to be 20 MWm^{-2} assuming that

(1) the convective power loss is 70% of the total heating power of 40 MW,
(2) the effective width of the strike zone is 4 cm
(3) the asymmetry in the heat flux between inner and outer strike zone is 2:1.

The convective power loss of 70% was obtained in JT-60 with the TiC wall in a clean discharge of low radiative loss. The characteristics of the divertor plasma will be measured in this years experimental phase using of Langmuir probes, thermo-couple arrays, infra-red cameras, divertor bolometers, and H_α diagnostics.

The armour in the areas other than the divertor is fitted to the vessel wall by a single bolt in order to avoid sharing of induced eddy currents between the tiles and the vessel walls. Fig 5 shows across-section of the JT-60U vessel. The surface is divided into different areas, wall (A,B) and divertor (D). The design heat flux on areas A and B resulted from equilibrium calculations of the plasma configuration. The heat flux for the region A was found to be 3 MWm^{-2} and that for region B to be 1.5 MWm^{-2}. The tiles in region A were adjusted in such a way that steps between adjacent tiles are below 1 mm in order to avoid damage on the edges. The heat flux for these regions was estimated according to measured data for the scrape-off layer thickness [7].

2.2 MATERIALS AND SELECTION FOR JT-60

Since large quantities of the different materials are required for the first wall armour, the material types should range over several brands so as to be produced within a limited period. The selection of materials was based on an examination of their properties such as thermal and electrical conductivity, thermal expansion coefficient, Young's modulus and mechanical strengths [8,9]. Test results for the thermal conductivities are given in Fig. 6. for ambient temperature.The brands from A to C denote isotropic graphites and D to G carbon fibre composites. It is remarkable that these brands have conductivities higher than copper. The temperature dependence of the thermal conductivity is shown in Fig. 7. While the values decrease with an increase of the temperature, most of them still have considerable conductivities at 900 K. Considerable anisotropy for these data was observed. The mechanical strength was found not to be higher than the one for isotropic graphites, and also showed some anisotropic characteristics. From these results and from the sizes that can be produced, the tile shapes and tile arrangements, as shown in Fig. 8, were determined.

2.3 FUTURE PLANS FOR JT-60

In the short term, it will be necessary to adjust the height difference of internal tiles after some period of operation. Following the experience at the original JT-60, the adjustment over a considerable area might be required. The surfaces of the divertor tiles are planned to be shaped to have a slight inclination towards the direction of the incident plasma so as to prevent plasma particles from directly impinging on the tile edges. This is an experimental test to suppress excessive sublimation of carbon during long periods of high power heating experiments.

For a middle term plan, boronization of the tiles and the use of boronized graphite are considered. The material studies have just started. On the other hand the

divertor might be changed to a closed configuration which was originally included as an option in the new vessel design. This option aims to improve the plasma purity. If this is adopted limiter discharges become much more difficult to set-up, therefore the wall armour, other than for the divertor,would be changed to materials like TiC.

In a long term plan, JT-60U would introduce high energy negative neutral beams [10]. This system would enable us to produce high temperature diverted plasmas at high density. In such a case the experimental plan will concentrate on the divertor plasma with closed configuration and we could abandon high power limiter discharges. As an option the divertor plate could be changed to a metal plate with forced cooling in order to cope with the high heat flux of the plasma. The technical problem of introducing water cooling lines into high temperature vessel will be solved in an early phase of JT-60U.

3. OPERATIONAL EXPERIENCE IN DIII-D

The DIII-D tokamak has a 'Dee' shaped cross-section with minor and major radius of 0.67 and 1.67 m respectively and a toroidal magnetic field $\leq$ 2.2 T. DIII-D is a versatile device capable of producing many plasma discharge shapes including upper null, lower null, or double null poloidally diverted discharges, inside wall limited discharges, outer limiter discharges and biased diverted discharges. Biasing is accomplished with a toroidally continuous insulated ring (installed in 1990) which can induce poloidal currents in the outer region of the plasma discharge. Auxiliary-heating power includes neutral beam injection (NBI) with hydrogen, deuterium, or helium atoms, $P_{NBI} \leq 20$ MW, electron cyclotron heating (ECH), $P_{ECH} \leq 1.7$ MW, and ion cyclotron heating (ICRH), $P_{ICRH} \leq 2$ MW into hydrogen, deuterium, or helium plasmas. A detailed description of the DIII-D tokamak is presented in reference 11.

Plasma discharge durations of ~ 10 s have been obtained [12] and auxiliary heating energy up to 50 MJ has been applied on a single pulse. Both average power density, $P_{aux}/V_{plasma} \leq .95$ MWm^{-3}, and ratio of auxiliary power to wall area, $P_{aux}/A_{wall} \leq$ 0.25 MWm^{-2}, are comparable to, or higher, than other large tokamaks presently operating, e.g. JET, TFTR, and JT-60.

3.1 DESCRIPTION OF DIII-D WALLS

DIII-D began operation with 7.5 m^2 of graphite corresponding to 9% of the plasma facing surface area. These graphite tiles were located in regions of high heat flux; the floor (for lower single null diverted discharges) and areas exposed to neutral beam 'shinethrough'. In addition two graphite limiters were located at the outboard midplane and spaced 180^o toroidally. Graphite was chosen for these high heat flux regions because of its low atomic number (Z = 6) and its ability to withstand high heat fluxes and thermal stresses. POCO AXF-5Q graphite was initially used primarily because of its high coefficient of thermal expansion which was compatible with the brazing process used to fasten the graphite tiles to the Inconel base [13]. However several of these tiles exhibited graphite fracture or separation from their metal

substrate and in one case this failure occurred during a machine opening with no external heat or mechanical loads on the tile. In order to reduce tile failure and expand the operating parameter range of DIII-D, graphite coverage was increased to 31 m^2 or ~ 40% of the plasma facing surface including the top, inside wall, and floor of the vacuum vessel as shown in Fig. 9 and the method of attaching the graphite tiles was changed from brazing to mechanical clamping.

All areas of DIII-D which can be exposed to high heat flux are now covered with graphite tiles. The armour consists primarily of ~ 1600 graphite tiles, Union Carbide type UCAR TS-1792. This type of graphite was selected based upon its low thermal expansion coefficient, high thermal conductivity, resistance to thermal and mechanical shock, and availability. Before selection, seven candidate graphite materials were tested at high heat flux in the Sandia National Laboratory Albuquerque (SNLA) ion and electron beam high heat flux facility and 3-D analysis was performed on the tile design to ensure that they would not fail due to localized thermal or mechanical stress [14].

For the large area graphite coverage shown in Fig. 9 the graphite tiles are secured to the Inconel 625 vacuum vessel with Inconel studs welded to the wall. The method of attachment is depicted schematically in Fig. 10 a. The graphite tiles are mechanically secured to the Inconel wall. Tile edges are overlapped to shield the metal components from direct plasma exposure (Fig. 10 b). The vessel wall has water cooling channels and thermal contact between the wall and the tiles is maintained with a copper foam material. The thermal limits for vessel wall stress, tile stress, and tile surface temperature of 2200 C is shown in Fig. 11. For the heat flux test performed at SNLA, TS-1792 exceeded the flux limits shown in the cross-hatched region shown in Fig 11 with no mechanical failure [14]. The operating region shown in Fig. 11 is compatible with DIII-D operations although the heat flux to the divertor tiles is localized and not evenly distributed over the surface of the tile. For example, a 20 MW diverted discharge with 30% of the input power conducted to the inner and outer divertor strike points would produce a power flux of 10 MWm^{-2}. It is assumed in this example that the heat flux peaks at the centre of the strike point and the strike points consist of 'stripes' toroidally symmetric on the floor. The width of these stripes is assumed to be 2 cm at full width half maximum of the heat flux, which is consistent with experimental observations. Because this heat flux is localized, and not distributed over the entire surface of the tile, 3-D calculations show that the tile can sustain a flux of 10 MWm^{-2} for 10 s, or more than 4 times as long as the 2.4 s which would be estimated from Fig. 11. The peak divertor energy and heat fluxes in DIII-D have been measured with an infra-red camera and are ≤ 6 MJm^{-2} and < 5 MW/m^{-2} respectively [15].

In addition to the graphite tiles described previously, boron nitride (BN) insulating tiles were installed in 1990 as part of the advanced divertor project. These tiles insulate a toroidally symmetric ring which can be biased with respect to the rest of the vessel to drive poloidal electric currents in the edge region of the plasma discharge [16]. As shown in Fig. 12, flux surfaces from the scrape off layer intersect the boron nitride tiles and these tiles can be subjected to high heat fluxes. Boron nitride was chosen as an insulating material over other candidates materials such as SiC because of its non-catastrophic failure (sublimation) when subjected to high heat thermal

fluxes. The usual failure mode of SiC, on the other hand, was cracking and shattering of the tile during high heat flux tests at SNLA [17]. The versatile field shaping system in DIII-D allows the positioning of the outer strike point or scrape-off layer either on the biased divertor ring or near the aperture below the ring as shown in Fig. 12. Plasma discharges are also routinely obtained with the outer strike point positioned at a smaller major radius to minimize any potential interaction with the ring or insulators.

Graphite and boron nitride tiles comprise 40% of the first wall area exposed to plasma discharges. The remaining parts of the vessel are either Inconel tiles or the Inconel vessel wall itself. All exposed metal surfaces are in areas of low heat flux where metal sputtering is expected to be minimal. Metal contamination in the plasma discharge can be a serious problem and, in fact, has been observed in DIII-D during high plasma current ($\geq$ 2 MA) high confinement mode (H-Mode) discharges [18]. The mechanism for this metal influx has not been determined. Possibilities include direct sputtering of the metal surfaces by charge exchange neutrals or transport of metal atoms to the graphite tiles during events such as disruptions or glow discharge conditioning of the vessel and the subsequent desorption of the metal atoms during a tokamak discharge. The deposition of a thin carbon film of ~100 nm (carbonisation) on all plasma facing surfaces has successfully reduced the metallic impurities as shown in Fig. 13. Nickel and oxygen fluxes are reduced by a factor of 5 to ~ 30 after carbonisation when compared to a similar plasma discharge before carbonisation. The fraction of radiated power was also reduced for comparable tokamak discharges.

3.2 OPERATIONAL EXPERIENCE WITH GRAPHITE TILES IN DIII-D

Large area graphite coverage in DIII-D allows high power ($\leq$ 20 MW) auxiliary heating with significantly reduced high Z metallic impurity contamination. Carbonisation further reduces metallic impurities. As a result the following important plasma parameters have been achieved: H-mode discharges up to 10 s duration, observation of limiter and ohmic H-mode confinement, 2.5 MA divertor operation without carbonisation and 3 MA divertor operation after carbonisation, more reliable low q operation, and volume averaged beta of 11% [12, 19]. It should be emphasized that this improved performance was accomplished only after careful conditioning of the graphite, as discussed later in this section. There has been no evidence of carbon blooms which have been observed in JET and TFTR. The maximum tile temperature in DIII-D is estimated to be ~ 1500 - 1700 C and occurs at the edge of tiles near an opening such as a port aperture [15].

One concern in designing high heat flux components for large tokamaks is that currents can flow through these components. Current monitors have been installed in DIII-D to measure currents conducted through the tiles both during current flat top and during disruptions [20]. As shown in Fig. 14 the current flowing in the tiles during a disruption can be a significant fraction of the total plasma current [21, 22] before disruption. Calculated poloidal currents are in good agreement with currents measured by tile Rogowski loops (from [22]). These tile currents create $\bar{j} \times \bar{B}$ forces which can damage the tiles or tile support structures. However no structural damage from disruptions to either the graphite tiles or their attachments has been observed in

DIII-D. The currents flowing in the vessel structure have been measured, and a model has been applied to characterize the disruption forces [21, 23].

Conditioning of the graphite is critical in obtaining high performance plasma discharges. Graphite is a reservoir for trapping hydrogen with concentrations of hydrogen to carbon atoms, H/C of ~ 0.4. During a tokamak discharge some of the particles in this reservoir can be desorbed from the walls. Hence even if the graphite tiles are 'cleaned', i.e. no oxygen or loosely bound carbon to contaminate the discharge, there can still be a large and often unwanted fuelling source of hydrogenic particles. DIII-D has applied a technique of helium glow wall conditioning (HeGWC) before every tokamak discharge in order to lower the hydrogen concentration in the surface regions of the graphite The application of this repetitive HeGWC has been successful in conditioning the graphite and controlling the wall fuelling [19].

Although auxiliary heating energies up to 50 MJ per discharge have been applied, there has been no major damage to high heat flux plasma facing components since the installation of large area graphite coverage. There have been small areas of localized melting around the edges of some plasma facing Inconel surfaces and in the neutral beam drift ducts which connect the neutral beam injectors to the main vacuum vessel. The cause of this melting is not well understood, but substitution of graphite for Inconel in some areas and changes in operating procedures such as more time for drift duct conditioning of the neutral beam injectors has reduced the incidence of this melting. The high heat flux boron nitride insulation tiles have not shown any signs of damage in the first 6 months of operation. In general, the DIII-D experience with graphite and boron nitride has been quite successful. However there have been some ancillary problems. For example, copper 'bursts' are periodically observed in DIII-D discharges and these bursts can occasionally cause a deterioration in plasma confinement (locked modes) or premature termination of the discharge (disruptions). The source of this copper injection is the copper foam material used to provide thermal contact between the tiles and the vessel wall (Fig 10 a). Small pieces have periodically detached from the foam and fallen into plasma discharges. This problem has been minimized by careful cleaning and substitution of a copper 'felt' material whenever tiles are removed (primarily for diagnostic access) during a vessel opening. The frequency of copper bursts has decreased in the three years since the tiles were first installed and is not a serious impediment to operation.

In conclusion, graphite has been successfully used as the primary high heat flux material in DIII-D. Boron nitride insulating tiles have also been installed in DIII-D to insulate a biased divertor ring used to drive poloidal currents in the scrape-off layer of the plasma. Conditioning of the graphite tiles, consisting primarily of HeGWC, has allowed routine operation with heat fluxes as high as 6 MWm^{-2} and has expanded the the parameter space in which DIII-D can operate.

4 OPERATIONAL EXPERIENCE IN JET

The Joint European Torus (JET) is the central and largest project of the fusion programme of the European Community. This programme is coordinated by the European Atomic Energy Community (EURATOM).

The JET objective is to obtain and study a plasma in conditions and with dimensions approaching those required in a thermonuclear reactor [24]. Deuterium tritium (D-T) mixtures will be used to study the production and confinement of alpha particles generated by fusion reactions and the subsequent heating of the plasma. Technical aspects of and progress towards D-T operation at JET have already been reported [25, 26, 27].

4.1 WALL MATERIALS USED IN JET

Since the start of JET operation in 1983, a large effort has been made to reduce plasma impurities and their impact on plasma performance [28]. The first wall consisted initially of high-Z material (Nicrofer 7612 similar to Inconel 600). After frequent damage of the high-Z material by runways the walls were protected by graphite tiles and remaining metallic surfaces were covered with hyrogenated carbon films (carbonisation). Graphite tiles were also used for limiters and X-point target plates [28,29]. Operation with a carbon first wall was successful. The plasma current was raised to 7 MA, at low plasma current (3 MA), quasi steady state operation was achieved with T_i and T_e above 5 keV for 20 seconds and in H-mode discharges a value of 2.5×10^{20} m^{-3} keVs was obtained [30] for the fusion parameter ($n_D T_i \tau_E$).

With a carbon first wall, performance was limited by impurities, mostly carbon and oxygen, coming from the walls. This is reflected by the plasma dilution (ratio of deuterons to electrons) which will be about 0.6 even with moderate heating power in the range of 5 to 10 MW. Carbon impurities coming from the graphite walls decrease the fusion yield by diluting the the fuel, increasing the radiated power, and decreasing neutral beam penetration. The carbon influx increases rapidly as soon as the surface temperature of graphite elements in contact with the plasma reaches 1200-1300 C This is mainly due to radiation enhanced sublimation and self-sputtering which can increase the carbon influx in an avalanche-like process [31]. This effect, called at JET the "carbon catastrophe", results in a sharp decay of the fusion parameter.

Beryllium was then proposed to replace graphite as a first wall material because of its lower atomic number, its chemical resistance against hydrogen and its gettering properties for oxygen. A comparison between carbon and beryllium is given in [32]. Also preparatory experiments in ISX-B [33] and UNITOR [34] indicated that beryllium was a viable limiter material. Beryllium was first introduced into JET in 1988 and has been used with great success since.

Physics results and technical aspects for the beryllium operation are given in references 35-37. The main effects have been the reduction of plasma dilution, the enhancement of wall pumping the increase in sustainable density and the absence of density limit disruptions. From the improved plasma purity, an improvement of nearly all plasma parameters ensues and the fusion parameter increased to values of 9×10^{20} m^{-3}keVs. This is very close to breakeven in a deuterium tritium plasma.

The effect on impurities is demonstrated in Table 2 which gives typical impurity concentrations and the dilution for the carbon phase (carbon first wall), the Be/C phase (beryllium evaporation on graphite walls and limiter), and the Be phase (Be limiter, graphite wall, graphite X-point tiles, Be evaporation).

A schematic of JET is shown in Fig. 15 for a Double Null X-point discharge with the strike zones on the upper and lower X-point tiles. The toroidal limiters [38], which are not used in this configuration are at the outboard side of the vessel. The inner wall shows a discontinuity above and below the equatorial plane because internal saddle coils which will occupy this space, have not been installed yet They will be used for the stabilisation of plasma disruptions [29]. Installation is planned for 1992.

The inboard wall is covered with graphite tiles. In the equatorial plane over a height of ±1 m where the heat load is highest during normal operation and plasma disruptions, the tiles are made of CFC. They have been aligned within ± 2 mm and can act as an inner bumper limiter with a power handling capability of 400 MJ. Useful plasma discharges with an acceptable plasma dilution can, however, only be sustained at much lower levels. Observations of the tiles showed that even though most tiles remained at temperatures below 600 C, some were heated sometimes up to 3000 C. Carbon sublimation often leads to increased impurity influxes and plasma disruptions. Energy inputs above 20 MJ were sufficient to produce this effect.

Then X-point protection consists of 32 poloidal rows of CFC tiles which were shaped and aligned to minimise local hot spots on the tiles. The leading edge of each tile is shadowed by the adjacent tile. Sweeping of the X-point has been carried out in order to increase the effective area. With sweeping and injection of gas into the X-point region the carbon influx could be delayed, 5.3 s long H-mode discharges could be sustained and 30-40 MJ per pulse could be deposited on these tiles before the onset of the "carbon catastrophe".

After a temporary replacement of the bottom protection by beryllium during 1990, presently new continuous X-point dump plates [29] are being installed with graphite fibre tiles at the top and beryllium tiles at the bottom of the machine. It is expected that the impurity ingress will be delayed during operation with the new X-point dump plates. They have a much larger surface than the existing X-point tiles and will follow very closely the theoretical shape of the torus in both the toroidal and poloidal directions. Toroidal steps on the beryllium plates are smaller than 0.1 mm. This is achieved by shading leading edges with the penalty of reducing the power handling capability.

The belt limiter forms toroidal rings above and below the equatorial plane of the machine, at the outboard wall [38]. Tiles in contact with the plasma are radiatively cooled and are held in watercooled supports. They can be easily exchanged. The beryllium employed is S-65B, cold pressed and sintered. The front face of the beryllium tiles is castellated in order to avoid the deep propagation of surface cracks. The belt limiter was designed with a power handling capability of 40 MW for 10 seconds. The design value of the peak heat flux was 5 MWm^{-2}. The observed peak heat flux in operation was more than one order in magnitude higher due to uneven loading between the top and bottom belts, scrape off thickness smaller than assumed and edge loading of the tiles. This resulted in localized melting and thermal cracking of about 5% of the plasma facing area [39].

Melting of beryllium tiles was only superficial and did not affect the tile integrity or operation although surface unevenness of about ±1 mm was observed in some areas. The energy deposition on the belt limiter has generally been kept well below the design value of 400 MJ. With a careful selection of the plasma shape so as to maximise the plasma foot print on the limiter and tailored gas feed during discharges it has been possible to apply in the best cases 180 MJ of heating energy at Z_{eff} values of 1.5.

4.2 PROBLEM AREAS FOR JET

The operation with high-Z walls showed runaway damage which occurred during disruption at runaway energies of about 30 MeV and currents in the MA range [28]. Protection of the affected areas with fine grain graphite resulted in an improvement, but still the material failed occasionally. Replacement by carbon fibre reinforced graphite eliminated the problem and runaway discharges of several seconds durations at energies in excess of 50 MeV at currents of several MA can be sustained without gross mechanical failure.

Eddy current forces due to the current quench during disruptions have never been a problem. Their impact on first wall components was analysed during the design phase of these components and resulting forces and moments and were taken care off in the design.

Lately, as the stored energy in the plasma increased, a new failure mechanism was found, which leads to severe damage of inner wall components. The plasma can move vertically as consequence of a vertical instability. Poloidal currents (halo currents) can be scraped off by in vessel components which are touched by the plasma when it comes into contact with the vessel. They flow through the wall protection in poloidal direction. Their interaction with the toroidal field leads to high forces and, depending on the design, to huge moments. Fig. 16 shows an example of damage to the inner wall protection where a carbon fibre reinforced graphite tile was ripped off its support. The area of this tile is about 0.15 x 0.15 m^2 and the force required to cause this type of damage was in excess of 500 dN as evaluated from a post mortem analysis of the tile. Presently the design of all components built or going to be built into the vessel is undergoing a review with the aim to eliminate possible damage due to halo currents.

4.3 FUTURE PLANS FOR JET

The results described above were only achieved in transient conditions. The high quality period of a plasma pulse lasts only for a second or less, and the D-D neutron count, which is a measurement of fusion performance decays rapidly as impurities penetrate the plasma. Even if this time can be increased with the new dump plates, this approach is not relevant for the machines of the next generation which will operate for long pulses, a few 100 to a few 1000 seconds, and therefore require steady state conditions for the plasma and active cooling of the HHF components.

It is also necessary to obtain more data on the operation of divertor systems required for the next step devices. The problems of controlling the back-flow of impurities from the divertor target to the plasma and of the target plate erosion have never been studied experimentally with plasma parameters and pulse durations which are of some relevance for next step machines. Due to its size, plasma performance and long pulse capability, JET is in a unique position to carry out such studies and the installation of a Pumped Divertor is proposed .

The basic aims [31,40] of the Pumped Divertor are to reduce the power load on the divertor plates by increased radiation from the divertor throat, to screen the target plates from energetic plasma particles and therefore to decrease the impurity production and to impair the impurity transport into the plasma.

Technical aspects of the Pumped Divertor are given in [41]. Fig. 17 shows an example of a configuration of the JET Pumped Divertor for a Single Null plasma with 5 MA current. The main components are:

- The divertor coils which produce the required magnetic configuration.
- The target plates.
- The cryopump which will help in controlling the main plasma density.

The target plates are made up of three parts. The horizontal plates intersect the heat flux conducted along field lines while the vertical side plates receive the radiated power from the divertor target plasma. The plates are segmented toroidally into 384 elements.

Initially the plasma facing material will be radiation cooled beryllium with a capability of handling about 100 MJ. At a later stage actively cooled target plates for a total steady state conducted power of 40 MW will be employed at the bottom. The average power flux density will be about 12 MWm^{-2} when sweeping of the X-point is taken into account [42]. Peak loads are in the range of 50 MWm^{-2}. These power densities require the use of highly efficient heat sinks. Hypervapotrons are selected which have been used extensively for the JET Neutral Beam systems and can cope safely with steady state heat fluxes up to 25 MWm^{-2}. The side plates may receive up to 5 MWm^{-2} in case the full power is radiated by the divertor plasma.

The hypervapotrons, consisting of a copper-chromium-zirconium alloy, will be clad with a 3 mm thick beryllium layer. The choice of beryllium is supported by the results achieved with a beryllium first wall in JET. It is not ideal since beryllium in the divertor plasma will only radiate a negligible fraction of the incident power. The choice of another material with a higher Z (e.g Silicon) would however entail the risk of high-Z impurities migrating back to the vacuum vessel walls and wipe out the benefits of a beryllium first wall.

The bond strength between the beryllium cladding and the hypervapotron is critical. Silver brazing at about 650 C is a preferred method of joining but the strength of the bond is strongly reduced when the operating temperature exceeds 350-400 C. An active braze is presently under investigation and shows so far promising results.
Analytical studies have shown that an average flux density of 12 MWm^{-2} and a sweeping frequency of 4 Hz give acceptable temperature excursions for both the beryllium surface and the beryllium copper interface. To avoid hot spots, particularly

at the edges each segment is tilted so that the edge is shadowed by the adjacent segment. All segments will have to be aligned with respect to each other within ±0.25 mm. The beryllium layer should be castellated to minimise the plastic strain. This can be achieved by brazing small tiles with dimensions of 6-10 mm.

Large forces can act on the hypervapotrons due to currents flowing during disruptions. Some eddy current paths have been eliminated by a careful design of the mechanical attachments. During vertical instabilities halo currents could be shared between the vessel and the hypervapotrons. Forces of up to 2 tons per metre could be produced on each of the 384 toroidal elements, which, to resist these forces, are firmly clamped onto steel beams which themselves are attached to the lower divertor coils.

4.4 OUTLOOK FOR JET

Impurity control at JET has so far concentrated on the development and use of passive elements such as low Z materials for wall protection, limiter tiles and X-point target plates. Graphite and more recently beryllium have been used with great success but impurity influxes prevent the attainment of higher performances and steady state conditions.
A new Pumped Divertor configuration is proposed for JET which would address the problem of impurity control in operational conditions close to those of the next generation of machines. The construction and operation of the JET Pumped Divertor requires an extension to the JET Experimental Phase. It is planned that installation would take place in 1992 and operation with the Pumped Divertor would start in 1993. This extension if approved will allow essential data to be obtained on the operational domain of next step machines, the physics of the divertor and technological aspects such as the choice of materials facing the plasma.

5. TFTR OPERATIONAL EXPERIENCE

TFTR is a tokamak with a circular cross-section. The major and minor radii are 2.45 to 2.62 m and 0.80 to 0.96 m respectively with a current capability of up to 3.0 MA. Its main aim is to investigate reactor like operation regimes and to produce a level of fusion power output comparable to the heating power input. The heating methods applied are Neutral Beam (36 MW maximum) and Ion Cyclotron Resonance heating (ICRH, 14 MW maximum). The maximum pulse duration of the heating power is two seconds.

5.1 DESCRIPTION OF THE DESIGN OF THE TFTR PLASMA FACING MATERIALS

The TFTR bumper limiter is a toroidally axisymmetric structure that subtends 120° in the poloidal direction. It is located on the small major radius side of the torus. The surface area of the bumper limiter is about 20 m^2. The surface is composed of about 1928 graphite tiles mounted on Inconel 718 backing plates. The backing plates are cooled by water. The limiter is divided into 20 assemblies (bays) arranged in groups of 3 (upper, lower and centre plates, see Fig. 18). The centre plate subtends 60° in the

poloidal direction while the upper and lower plates subtend only 30°. Because of disruption induced eddy current forces, the backing plates had to be cut as shown in Fig. 18. The cuts increase the electrical resistance of the plates and thereby reduce the maximum value of the eddy currents. This reduces the stress in the backing plates, but increases the deflections of the individual tile mounting sections. The location and number of cuts in the backing plates were determined from a compromise between reducing the stress and limiting the deflection. The left and right halves of the backing plates are electrically isolated but structurally connected using a bolted joint incorporating Mica Mat insulators and Macor bushings. This also reduces the magnitude of the eddy currents due to disruptions. Even with these measures, it was still necessary to invoke the affect of magnetic damping to obtain an acceptable design [43]. Magnetic damping is the reduction of the deflections and dynamic stresses, due to the motion of the facets of the backing plate, caused by the poloidal field eddy currents, resulting in a toroidal field eddy current, which damps the poloidal field induced motion.

The shape of the plasma facing surface of the graphite tiles was determined by a desire to prevent exposure of edges of tiles facing in the heat flux direction. To accomplish this goal, the toroidal radius of curvature of each row of tiles was made slightly less than the local major radius, i.e. the tiles at the edge of each backing plate are recessed about 2 mm from a true toroidal surface. In the poloidal direction the tiles are flat, which results in a shielding of the poloidal edges of the tiles from direct plasma bombardment. These efforts to shield the tiles from near normal incidence of plasma heat flux nearly double the peak heat flux, but avoid a peaking factor of about 100 due to exposed edges. The poloidal faceting also simplified the tile machining since only a cylindrical surface had to be made. The columns of tiles at the edges of the backing plates overhang the Inconel plate to prevent line of sight along magnetic field lines between metal surfaces. This was necessary because of the bellows (electrically resistive sections) in the TFTR vacuum vessel, which have a resistive voltage drop of about 180 V induced by disruption eddy current flowing the vacuum vessel. Studies conducted on PDX showed that no arcing was observed between graphite tiles separated by 3 mm toroidally with a bias voltage of 180 Volts [44]. There was not any damage observed on the edge of graphite tiles due to arcing.

In order to protect the ICRH antennas from plasma heat flux a set of RF limiters was installed. The RF limiter consists of two poloidal rings having a toroidal width of 0.5 m (see Fig. 19). Each ring is composed of 24 self-supporting (CFC) tiles made from a BFGoodrich 2D material. The tiles are cooled only by radiation to the vacuum vessel wall except at the outer mid-plane where there are water cooled radiation heat sinks. The leading edges (where the tile becomes normal to the magnetic field) of the RF limiter tiles in the toroidal direction are recessed 20 mm from the apex of the tile.

5.2 MATERIAL TYPE AND SELECTION FOR TFTR

During the design of the bumper limiter, TiC coatings were being seriously considered as a coating for plasma facing surfaces. A graphite that was compatible with TiC coatings was chosen for the bumper limiter tiles to allow for coating if TiC proved to be useful. POCO graphite was the material judged to be most compatible with TiC

coatings. The results of test of TiC coatings revealed serious plasma contamination problems due to spalling of the coating [1]. The POCO graphite tiles were installed without coating because of those results. Thermal analysis of the surface temperature rise due to the expected heat flux showed maximum temperature of about 1200°C. The energy from the plasma is stored in the heat capacity of the graphite during the discharge. The heat is removed from the graphite tiles between plasmas by conduction through the backing plates to water tubes on the back of the Inconel plates. The equilibrium starting temperature just before a plasma was calculated to be about 150°C for 100 MJ of heating. Equilibrium temperatures of about 80-90°C are observed with up to 50 MJ of input energy.

Damage of the POCO graphite tiles due to disruptions has lead to the replacement of about one third of the POCO tiles (see Fig. 20) with (CFC) tiles. These CFC tiles were made from a 4D composite from Fibre Materials Inc. The shape of the tiles and the backing plates was not changed when the CFC tiles were installed. The CFC tiles have about 20% higher thermal conductivity and about 10% higher density than the POCO graphite tiles.

The 2D CFC material was chosen for the RF limiter because it could be moulded into nearly final shape. It could also be made self-supporting, which greatly reduced the eddy currents and forces during disruptions. The elimination of the backing plate made the cost per unit area of the self-supporting design similar to the POCO graphite tile/Inconel backing plate design of the bumper limiter.

5.3 LIMITER PERFORMANCE IN TFTR

Alignment: When the bumper limiter was installed in TFTR, magnetic measurements were made to determine the location of the tiles with respect to the toroidal field. The measurements were made using Hall probes. An overall accuracy of about ± 2.5 mm was achieved. Only the centre backing plate was magnetically aligned. The upper and lower plates were aligned relative to the centre plates by mechanical means, but the alignment accuracy was not determined.

The RF limiter was aligned by mechanical measurements from the bumper limiter and vacuum vessel. It is vertically centred about the mid-plate to an accuracy of about ± 2 mm.

Erosion: Substantial localized damage of the POCO graphite tiles has been observed. Six tiles were found to be broken after the first long neutral beam heating experiments at high power. An additional 100 tiles were found to have surface damage. The surface damage was either cracking or spallation. There was a strong correlation between the tile damage and the high spots found in the limiter shape [45]. In several cases the damage was on the edge of a tile facing the heat flux because of local misalignment of that tile relative to its neighbours. The areas with the most severe spallation damage were found to contain Be^7 made by (e,γ,n,α) reactions due to impingement of run-away electrons created during disruptions. The erosion in the disruption damaged areas was up to 1.5 mm. The edges of depressions in the limiter

surface made for plasma diagnostics also showed severe erosion. No damage was observed on the CFC limiter tiles.

Surface Temperature: The maximum observed surface temperatures are about 3000 C. These high temperatures are limited to the disruption damage areas at the high spots on the limiter, misaligned tiles, and the edges of depressions in the surface made for diagnostics. The spalled areas on the surface of the tiles are observed to reach temperatures of about 1800°C with 25 MW of neutral beam heating for 1 s. The very high temperatures in the damaged areas cause a large influx of carbon into the plasma, which has come to be called a "Carbon Bloom" [46].

Surface temperatures of up to 3000 C have been observed on the leading edges of the RF limiter tiles. This is primarily due to the vertical elongation of low beta large major radius plasmas. At high beta the plasma becomes horizontally elongated and the high temperatures are not observed. Carbon blooms are observed in large major radius plasmas due to high temperatures on the RF limiter tiles.

5.4 PLASMA PERFORMANCE IN TFTR

The plasma performance was limited by "carbon blooms" at high beam power with POCO graphite tiles as the plasma facing material. This was due to the high temperatures in the disruption damaged areas and the exposed edges of misaligned tiles. The details of the "carbon bloom" phenomenon are discussed in ref. 46 and 47. Replacement of the POCO graphite tiles with CFC tiles and alignment of the mid-plane portion of the limiter resulted in elimination of "carbon blooms" except for very large (>2.6 m major radius) or very small plasmas (<2.3 m major radius). In both cases the blooms are likely due to the non-aligned regions of the limiter since high temperatures are still observed at the edges of tiles. The change of tile material to CFC has eliminated the disruption damage. Alignment of the mid-plane portion of the limiter has reduced the peak heat flux on the tiles. These two changes have eliminated the carbon bloom except for transient events or high power small minor radius plasmas and very large minor radius operation near the RF limiters [47]. Changes being made now will eliminate the problems in large and small major radius plasmas.

Plasma performance has also been improved by reducing carbon influx with lithium pellet injection. When a lithium pellet is injected after the beam heating in one pulse and before the beam heating in the next pulse, the performance of the second pulse is about 15% better than a similar sequence of plasmas without any lithium pellets [48]. The most significant change in the plasmas is a reduction in the carbon content of the second shot in the sequence. Before lithium pellet injection, a correlation was observed between plasma performance and the carbon content before beam heating, but it was not possible to control the carbon content in a given discharge. The lithium pellets have given partial control over the carbon content of the plasma. The reduced carbon levels last for only about 2-3 shots after lithium pellet injection is stopped. The mechanism responsible for the reduction in carbon content is not yet understood.

5.5 PROBLEM AREAS FOR TFTR

The carbon content of the plasma before neutral beam heating is still limiting plasma performance. This is due in part to the misalignment of the tiles on the limiter. Temperatures of about 1500°C are observed on tile edges. This temperature is probably only a lower bound because of the poor view of the edges of the tiles by the infra-red television system. In addition, the upper and lower portions of the limiter are not aligned to the accuracy of the mid-plane portion. This also leads to high temperature regions.

The hydrogen content of the TFTR plasma can be as large as 10% even after boronization with deuterated diborane. This is probably due to either water vapour influx from the neutral beam lines or diffusion from the bulk of the graphite (which contains about one atomic percent H).

Large major radius plasmas ($R > 2.55$ m) are limited in performance by carbon bloom effects and high metal content. The carbon blooms are due to the limited area of the existing RF limiters. The metal content is due to the proximity of metallic vacuum vessel structures to the plasma edge. Both of these issues will be addressed when the RF limiter upgrade is installed in March 1991.

5. 6 FUTURE PLANS FOR TFTR

The limitations on plasma performance due to the limited area of the RF limiter will be reduced by adding 6 additional segments (covering 90° poloidally on both top and bottom of the torus) of RF limiter. These segments will be installed during the winter 1990-91 opening. The new segments are identical to the existing RF limiter segments. The upgrade will increase the power handling capability of the RF limiter from 25 MW for 1 s to 50 MW for 2 s. In addition, the new segments will protect the metal portions of the vacuum vessel from plasma bombardment. This should reduce the metal content of the large plasmas.

The edges of the bumper limiter tiles that face into the heat flux will be tapered to prevent exposure of the leading edge with the measured misalignement of the tiles on a single backing plate. The taper is 5° with a depth of 1 mm. This will result in an increase of about a factor of 2 in the surface heat flux compared to the ideal heat flux with no tapering, but it will eliminate the peaking of about 100 in the heat flux due to near normal incidence on an exposed edge.

A careful magnetic and mechanical alignment of the entire bumper limiter will be done during the 1990-91 opening. This involves locating fiducial points in the vessel to an accuracy of ±0.1 mm using Nuclear Magnetic Resonance Probes. A measuring arm will be placed on the fiducial points and used to measure the position of 4 points on each (all 1928) bumper limiter tile. The arm has been constructed and found accurate to about ±0.25 mm. An overall alignment accuracy of better than ±0.5 mm is anticipated for each segment of the bumper limiter. The same system will be used to align both the existing and the upgraded RF limiter. This alignment should further reduce the peak surface temperature on the limiter tiles.

Studies are being conducted to find methods of applying boron to the limiter without using hydrogen containing gases. The methods being considered include boron pellets, boron evaporation, and sputter sources of boron. It is hoped the boron film on the limiter will reduce carbon erosion. Bulk boronized materials cannot be used because of the reduction in thermal conductivity caused by the addition of even a few percent boron to graphites. Boron is preferred to lithium coatings because of concerns about hydride formation with lithium.

TFTR is considering changing all the tiles in high heat flux areas on the bumper limiter to CFC. This would require changing an additional 630 tiles to CFC. Only minor damage is observed on the graphite tiles in these areas because disruption damage is concentrated at the inner mid-plane. Additional CFC tiles are not considered to be essential at this time.

6 TORE-SUPRA OPERATIONAL EXPERIENCE

TORE-SUPRA is a tokamak with circular cross-section. Its main aim is to study plasmas for pulse durations of up to one minute. Therefore superconducting toroidal coils and active cooling systems are used. The tokamak has produced 5900 shots since the start up in April 1988 and now operates routinely with plasma currents up to 1.8 MA at toroidal fields of 4 Tesla, electron densities from 1 to $5x10^{19}$ m^{-3} additional heating by ICRH of 4 MW for two seconds and LHH of 5 MW for the same time. Pulse durations range from 10 s flat top for ohmic discharges to current driven plasmas with LHH at 1.5 MW and 20 s plateau. All the plasma facing components are actively cooled for steady state operation and have been designed to remove additional power up to 25 MW (50% convective) through a pressurized cooling loop (3.5 MPa) operating with water at temperatures between 150 and 230 C. During operation all the different components are successively monitored with three infra-red cameras and continuously monitored with calorimetric measurements in the cooling loop.

6.1 WALL DESIGN FOR TORE-SUPRA

The inner part of the first wall is made of 36 independent sectors which are covered with 9000 brazed graphite tiles (7 x 2 cm^2). The 12 m^2 plasma facing graphite surface can sustain a steady state heat flux of 1.5 MWm^{-2} and remove up to 12 MW. After 3 years of mainly operating as a bumper limiter, less than 2% of the brazed tiles are fractured, mainly due to the relaxation of brazing internal stresses (1.5% were already fractured before the first plasma was produced). Plasma operation and disruptions have only damaged further 30 of the tiles [49]. The measured maximum mean power removed by this system is 1.5 MW. Separate calorimetric measurements have shown a toroidally non-uniform power deposition (illustrated in Fig. 21) with a maximum peaking factor of 2.4 in ohmic discharges. This misalignment results in heating preferentially the leading edges with a corresponding maximum incident heat flux of 0.9 MWm^{-2} for ohmic discharges. The additional power pulses are presently short enough to allow for safe operation until the inner wall position is corrected which will take place in September 1991. Power deposition during disruptions is often

localised in the same sectors which are misaligned and is concentrated on the equatorial plane

6.2 PUMPED LIMITER FOR TORE-SUPRA

Six pumped limiters of 3 different types are installed on TORE-SUPRA. They are designed for a particle removal rate equivalent to 60 mbarls^{-1} and for a power exhaust of 5 MW at an energy scrape-off length of 1 cm. One of the six limiters is instrumented and is a semi-inertially cooled horizontal pumped limiter, built by SNLA. The head (0.55 x 0.65 m^2)is made out of pyrolitic graphite blades and can remove 2 MW during a 7 s pulse. The throat entrance is located 35 mm behind the last closed flux surface. This limiter was installed in September 1988 and has sustained, with no major damage, plasmas with ohmic (1.5 MA, 2 x 10^{19} m^{-3}, 10 s) and LHH heating (4 MW, 3 s). Valuable information on recycling and the scrape off layer characteristics have been obtained with this instrumented limiter [50]. The maximum heat flux on the leading edge has been estimated to be 2.4 MWm^{-2} with a surface temperature always below 600 C. Infra-red surface imaging confirms that the design of the surface shape -based on calculated flux lines (including ripple) - was sufficiently accurate.

Two out of the six limiters are semi-inertially cooled vertical pumped limiters with 0.4 x 0.4 m^2 heads built with fine grain graphite. Surface temperature profiles measured during operation with ohmic and additional heated plasmas have shown that the energy scrape-off thickness in the vertical plane was similar to that of the horizontal one and had values, depending on operating conditions, between 1.0 and 1.5 cm. A maximum energy deposition of 2 MJ during a 10 s plasma shot (200 kW) with 700 C maximum surface temperature, has proven that this type of limiter is safe for operation during low power pulses.

The remaining three limiters are actively cooled vertical pumped limiters designed for continuous operation at a load of 700 kW with a maximum surface temperature of 1400 C under a 15 MWm^{-2} incident heat flux on the leading edge. They have been installed in the vessel and connected to the pressurized cooling lines in 1989. One of this type of limiters has been damaged during its first exposure in the plasma, for two reasons: Firstly a protruding part of a brazed tile cracked and the resulting loss of thermal contact led to localized overheating (> 2000 C), however with no marked sign of a carbon bloom. During the last vessel opening of the vacuum vessel, the protruding parts were repaired and aligned and today no overheating is visible. Secondly due to a lack of water flow during operation at 2 MJ the critical heat flux on one of the cooling tubes was exceeded and a water leak in the vessel occurred. A disruption followed and about a half litre of water was removed from the torus after the vessel opening.

Presently these pumped limiters are progressively moved inwards towards the last closed flux surface and detailed thermal analysis is carried out by infra-red imaging.

6.3 NEUTRALISER PLATES

Thirty actively cooled neutraliser plates are installed between the bars of the 6 ergodic divertor windings. They can each support in steady state operation a maximum heat load of 10 MWm^{-2} with a surface temperature of the brazed graphite tiles of 1000 C. Ergodic divertor operation has proven to be satisfactory and a maximum of 100 kJ was extracted by each of the neutralisers which corresponds to a 5 MWm^{-2} incident heat flux. All these elements have been replaced during the last vessel opening due to a generic leaking on a copper to copper electron beam weld. Since the restart of operation one brazed tile (over 30 observed) shows signs of a brazing defect. This should not have any impact on the divertor operation.

6.4 POLOIDAL LIMITERS IN TORE-SUPRA

Ten actively cooled poloidal limiters have been installed on the three ICRH antennae and the two LHH launchers. They can sustain a 10 MWm^{-2} continuous heat flux normal to the limiter surface at the tangential point with the plasma, resulting in a surface temperature of 1100 C. During plasma heating the ICRH protection limiters have removed over 150 kW with a surface temperature of 700 C. These values are close to those expected for the nominal operation regime of this protection and no abnormal behaviour has been detected up to now.

Due to the good behaviour of the plasma facing components, the upgrading of the additional power of TORE-SUPRA to a value of 10 MW before the summer of 1991 could be carried out without the need for modifications of the present first wall elements. A new generation of first wall and pump limiter elements are being studied.

7 SUMMARY AND CONCLUSIONS

Plasma performance is strongly dependent on the wall materials employed in the tokamaks. It became very early evident that for additional heated discharges only low Z materials can be used. This was again again emphasised by the findings in DIII-D before large area graphite coverage and more recently carbonisation, in JET with Nicrofer walls and in JT-60 with TiC coated molybdenum walls where it was found that high power high current discharges could not be sustained in a high Z environment. There has, however, never been a sustained effort to overcome the problems related to these materials. To make the use of high Z materials a viable proposal, there is more effort required in present machines and JT-60U intends to do research in this area.

Graphite is today the favoured wall material, in form of fine grade graphite for areas with moderate heat loads, and as carbon fibre composite for limiters or divertors. The high thermal conductivity of these materials make them ideally suited for coping with high heat loads in present day machines and operation benefits from the fact that graphite sublimates and and does not melt if thermally overloaded. On

the other hand plasma dilution by carbon (JT-60, TFTR and JET) is a serious problem. The high hydrogen retention makes density control difficult and special conditioning methods are frequently required in present day tokamaks operating with graphite walls (TFTR, DIII-D). For the Next Step devices with continuous operation a large tritium inventory can therefore be expected if graphite at low temperatures is used extensively. A further drawback is the fact that the thermal conductivity of graphite degrades already at very low neutron irradiation so that its use for high heat flux components in Next Step devices is restricted and alternatives have to be found.

Beryllium has performed well in JET, giving excellent plasma performance , good density control, low impurity content, and by using this material density limit disruption do not longer exist. Operation with beryllium , however, is delicate because it melts if overloaded. At high plasma densities melting does not lead to a degradation in performance.

It was emphasised by all large tokamaks, but clearly demonstrated by TFTR, that the alignment of the limiter surface is crucial and that steps have to be smaller than 0.5 mm. For divertor machines good alignment is as well necessary but due to impurity screening it appears to be less important at least for the pulse durations of DIII-D or JT-60. For long pulse machines alignments better than a fraction of a mm may be required which becomes impractical considering the dimension of Next Step devices. " Shadowing" of leading edges will have to be employed which requires a reasonable angle of incidence of the incoming particles. This technique has its disadvantages because it reduces the area in contact with the plasma and simultaneously the power handling capability.

Abnormal operating conditions have not presented major problems with respect to failure of wall components due to runaway damage or eddy current forces. Thermal overloading of wall components occurred during disruptions mainly in misaligned areas. Early problems could be eliminated with the introduction of CFC graphites in critical areas and improved alignment . There are, however, observations in DIII-D and JET which indicate that during vertical plasma movements during vertical instabilities currents are introduced in wall components which can produce large forces by interacting with the toroidal field. In JET poloidal currents of up to 1.5 MA (30% of the total) were observed which led to damage of wall components. The possible occurrence of such currents will have to be taken into account in the future for the design of wall components.

TORE-SUPRA is the only one of the large machines which employs heat removal systems which are relevant to Next Step devices. The surface temperatures of the high heat flux elements are in equilibrium with the plasma during discharges and stationary conditions can be achieved. In all other machines surface temperatures change with pulse duration and therefore no true stationary condition can be obtained.

Extrapolating from the results of the large tokamak to the Next Step devices, there still remain some questions to be answered. The main ones are:

- Can graphite be used as high heat flux material due to degradation in

thermal conductivity and the expected large tritium inventory? Can beryllium be an alternative?
- So far no tokamak could produce high performance plasma with high Z wall materials. Is such a scenario possible?
- During abnormal operation conditions, how is the power sharing between walls and divertor during energy and current quench?
- Where do runaways strike first wall components? Is there an inherent incompatibility with high-Z materials due to power deposition on their surfaces and resulting surface melting?

Following the results and the experience of the large machines with wall materials and designs there is now more confidence that the above questions can be addressed properly and that a solution will be found for the high heat flux components of the Next Step.

ACKNOWLEDGEMENT

The JT-60 contribution reviews work performed by the JT-60 team during the experimental phase, and by the JT-60 upgrade group during the design and construction phase. The author of this part of the publication would like to express his appreciation to Drs. I. Kondoh, H. Shirakata, Y. Tanaka and T. Iijima for their leadership and support.

The DIII-D contribution reported work which is supported by the US Department of Energy, contract No DE-AC03-89ER51114.

REFERENCES

[1] J. L. Cecchi, M. G. Bell, M. Bitter, et al., Initial Limiter and Getter Operation in TFTR, J. Nucl. Mat. 128 &129 (1984),1-9

[2] N. Hosogane, K. Shimizu, H. Shirai et al., High Ion Temperatures and Characteristics of High Z_{eff} Hydrogen Plasmas in JT-60 Limiter Discharges, Nucl. Fusion 28(1988)1781-1789

[3] T. Imai, K. Ushigusa, K. Sakamoto et al., Current Drive and Confinement Studies during LHRF Experiments on JT-60, Nucl. Fusion 28(1988)1341-1350

[4] T. Nishitani, K. Itami and K. Nagasima, Radiation Losses and Global Power Balance of JT-60 Plasmas, Nucl. Fusion 30(1990)1095-1105

[5] T. Sugie, K. Itami, H. Nakamura et al., Impurity Control and Helium Exhaust Experiment in JT-60, presented at the 13th Int. Conf. on Plasma Phys. and Contr. Nucl. Fus. Res., Washington D. C., USA (1990) and published in the IAEA proceedings

[6] H. Ninomiya, N. Hosogane, R. Yoshino et al., Physics Operations in JT-60, Kakuyugo Kenkyu, 65-Supplement (1991) 13-26 (in Japanese)

[7] P.C. Stangeby and G.M. McCracken, Plasma Boundary Phenomena in Tokamaks, Nucl. Fusion 30(1990)1225-1379

[8] T. Ando, H. Takatsu, M. Yamamoto et. al., Material Characteristics of Graphite First Wall and C/C Composite Divertor Plate for JT-60, Proc. Int Symp. on Carbon, Tsukuba (Japan) Nov. 1990

[9] M. Yamamoto, T. Ando, H. Takatsu et al., Evaluation Test on First Wall and Divertor Plate Materials for JT-60 Upgrade, JAERI-M 90-119, Aug. 1990 (in Japanese)

[10] O.A. Anderson, W. S. Cooper, W. B. Kunkel et al., Negative Ion Source and Accelerator Systems for Neutral Beam Injection in Large Tokamaks, presented at the 13th Int. Conf. on Plasma Phys. and Contr. Nucl. Fus. Res., Washington D. C., USA (1990) and published in the IAEA proceedings

[11] DIII-D program staff, General Atomics report GA-A19264 (1989)

[12] J. L. Luxon, G. Bramson, K. H Burrell et al., Recent Results from DIII-D and their Implications for Next Generation Tokamaks, presented at the 13th Int. Conf. on Plasma Phys. and Contr. Nucl. Fus. Res., Washington D. C., USA (1990) and published in the IAEA proceedings

[13] J. P. Smith, P. M Anderson, C. B. Baxi, E. E. Reis and P. D. Smith, Design of DIII-D Armor Tiles, Proc. 12th Symp. Fus. Engrg. 1(1987)144-150

[14] C. B. Baxi, P. M. Anderson, E. E. Reis, J. P. Smith and P. D. Smith, Thermal Stress Analysis and Testing of DIII-D Armor Tiles, Proc. 12th Symp. Fus. Engrg. 1(1987)231-234

[15] D. N. Hill, T. W. Petrie, J. N. Brooks et al., Divertor-Plasma Studies on DIII-D, presented at the 13th Int. Conf. on Plasma Phys. Contr. Nucl. Fus. Res., Washington D. C., USA (1990) and published in the IAEA proceedings

[16] M. A. Mahdavi, M. Schaffer, R. Stambaugh et al., Divertor Baffling and Biasing Experiments on DIII-D, presented at the 13th.Int. Conf. on Plasma Phys. Contr. Nucl. Fus. Res., Washington D. C., USA (1990) and published in the IAEA proceedings

[17] J. P. Smith, C. B. Baxi, E. Reis, M. Schaffer and G. Thurston, Design of DIII-D Advanced Divertor, Proc. 13th Symp. Fus. Engrg. 2(1989)1315-1318

[18] G. L. Jackson, B. L. Doyle, D. N. Hill et al., Wall Conditioning and Plasma Surface Interactions in DIII-D, Proc. 16th Symp. Fusion Technol., London (UK), September 1990, in publication

[19] G. L. Jackson, T. S. Taylor and P. L. Taylor, Particle Control in DIII-D with Helium Glow Discharge Conditioning, Nucl. Fusion, 30 (1990)2305-2317

[20] M. J. Schaffer and B. J. Leikind, Observations of Electrical Currents in Diverted Tokamak Scrape-Off Layers, General Atomics report GA-A20128 (1991) submitted to Nucl. Fusion

[21] E. J. Strait, L. L. Lao, J. L. Luxon and E. E. Reis, Observation of Poloidal Current Flow to the Vacuum Vessel Wall During a Tokamak Vertical Instability, General Atomics report GA-A20036 (1990), to be published in Nucl. Fusion (1991)

[22] A. G. Kellman, J. R Ferron, T. H. Jensen et al.,Vertical Stability, High Elongation, And the Consequences of Loss of Vertical Control, Proc. 16th Symp. Fusion Technol., London (UK), September 1990, in publication

[23] T. H. Jensen and D. G. Skinner, Support of the Model for "Vertical Displacement Episodes" from Numerical Simulation of Episodes Observed in the DIII-D Tokamak, Phys. Fluids B, 2 (1990)2358

[24] P.H Rebut , The JET Project (Design Proposal), Commission of the European Communities, EUR 5516 e (1976)

[25] M. Huguet and E. Bertolini, Main Features Implemented in the JET Facility for D-T Operation, Fusion Technol. 10(1986)1398-1403
[26] R. Haange, A. Bell, C. Caldwell-Nichols et al., General Overview of the Active Gas Handling System at JET, Fusion Technol. 14(1988)461-465
[27] T. Raimondi, The JET Experience with Remote Handling equipment and Future Prospects, Fus. Engrg. and Design 11(1989)197-208
[28] K. J. Dietz, Experience with Limiter- and Wallmaterials in JET, J. Nucl. Mat. 155-157(1988)8-14
[29] M. A. Pick, G. Celentano, K. J. Dietz et al., Integrated Design of New In-Vessel Components, Proc. 15th Symp. Fusion Technol. 1(1988)771-775
[30] R. J. Bickerton and the JET Team. Latest JET Results and Future Prospects, Proc. 12th Int. Conf. Plasma Phys. Contr. Nucl. Fusion Res. 1(1989)41-65
[31] P. H. Rebut, P. P. Lallia and B. E. Keen, Impurities in JET and their Control. Proc. 13th Symp. Fus. Engrg. 1(1989)227-235
[32] P. H. Rebut, M. Hugon, S. J. Booth et al., Low-Z Material for Limiter and Wall Surfaces in JET, JET-R(85)03
[33] P. K. Mioduszewski, P. H. Edmonds, C. E. Bush et al., The Beryllium Limiter Experiment in ISX-B, Nuclear Fusion, 26(1986), 1171-1192
[34] J. Hackmann and J. Uhlenbusch, Experimental Study of the Compatibility of Beryllium Limiters with Tokamak Plasmas, Nucl. Fusion 24(1984)640-642
[35] M. Keilhacker and the JET Team, Overview of Results from the JET Tokamak using a Beryllium First Wall, Phys. Fluids B2 6(1990),1291-1299
[36] K.J. Dietz and the JET Team, Effect of Beryllium on Plasma Performance in JET, Plasma Phys. Contr. Fusion 32(1990)837-852
[37] K. Dietz, M. A. Pick, A.T Peacock et al., Beryllium in JET, A report on the Operational Experience, Proc. 13th Symp. Fus. Engrg. 1(1989)517-521
[38] G. Celentano, G. E. Deksnis, R. Shaw, K. Sonnenberg and J. Booth, The JET Belt Limiter, Proc.14th Symp. Fusion Technol. 1(1986)581-587
[39] E. Deksnis, A. Cheetham, A. Hwang, P. Lomas, M.Pick and D. D. R. Summers, Damage to JET Beryllium tiles, J. Nucl. Mat. 176&177(1990)583-587
[40] M. Huguet, E. Bertolini and the JET Team, Technical Status of JET and Future Prospects, Proc. 13th Symp. Fus. Engrg. 1(1989)491-496
[41] M. Huguet and the JET Team, Technical Aspects of Impurity Control at JET: Status and Future, JET-P(90)70
[42] E. Deksnis, E. M. Garriba, D. Martin, C. Sborchia and R. Tivey, Design of High Heat Flux Components for the JET Pumped Divertor, Proc. 16th Symp. Fusion Technol., London (UK), September 1990, in publication
[43] D. W. Weissenburger, J. M. Bialek, G. J. Cargulia et al., Experimental Observation of the Coupling Between Induced Currents and Mechanical Motion in Torsionally Supported Square Loops and Plates, Fusion Technol. 10(1986)448-461
[44] D. K. Owens and R. Budny, unpublished data from PDX
[45] G. Barnes, D. K. Owens, G. D. Loesser and M. Ulrickson, Alignment of the TFTR Bumper Limiter, Proc. 13th Symp. Fus. Engrg. 2(1989)937-940
[46] M. Ulrickson, the JET Team and the TFTR Team, A Review of Carbon Blooms on JET and TFTR, J. Nucl. Mat. 176&177(1990)44-50
[47] A. T. Ramsey, C. E. Bush, H. F. Dylla, D. K. Owens, C. S. Pitcher and M. Ulrickson, Enhanced Carbon Influx in TFTR Supershots, PPPL Report PPPL-2071, Dec 1990, to be published in Nucl. Fusion

[48] J. Snipes, J. L. Terry, E. S. Marmar et al., Wall Conditioning by Lithium Pellet Injection on TFTR, to be presented at the 18th EPS, Berlin, Germany, June 1991
[49] D. Guilhelm, M. Chatelier, T. Evans et al., Ergodic Divertor Effects on Heat and Particle Fluxes in TORE-SUPRA, Abstracts 32nd APS Meeting, Division of Plasmaphysics, Cincinatti, Ohio, USA, November 1990
[50] M. Lipa, Ph. Chappuis and P. Deschamps, Brazed Graphite for Actively Cooled Plasma Facing Components in TORE-SUPRA, Description, Tests and Performances. Proc. 5th Carbon Workshop, Jülich, Germany, May 1990, to be published in Fusion Technology

Table 1

Typical impurity concentrations and radiation losses in JT-60 for divertor (outer X-point and closed configuration) and limiter operation. The subscripts e, C, Ti and O denote electrons, carbon, titanium and oxygen.

First Wall Configuration	Metallic Wall (TiC-Mo) Divertor	Limiter	Graphite Wall Divertor	Limiter
Z_{eff}	1.6	---	2.2	3-5
n_C/n_e (%)	0.2	---	0.8	4-9
n_O/n_e (%)	1	---	2	1-2
n_{Ti}/n_e (%)	0.006	---	$5X10^{-4}$ - $2x10^{-3}$	---
Radiation Loss (%) (Main Plasma)	10	> 60	15	20

Table 2

Impurity content (%) and dilution (on axis density ratio of deuterons to electrons) for typical JET discharges with different wall materials

	C Phase Limiter	Be/C Phase Limiter	Be Phase Limiter	Be Phase X-point
Oxygen (%)	1	0.05	0.05	0.05
Carbon (%)	5	3	0.5	1.5
Beryllium (%)	---	1	3	1
Dilution (n_D/n_e)	0.6	0.8	0.85	0.9

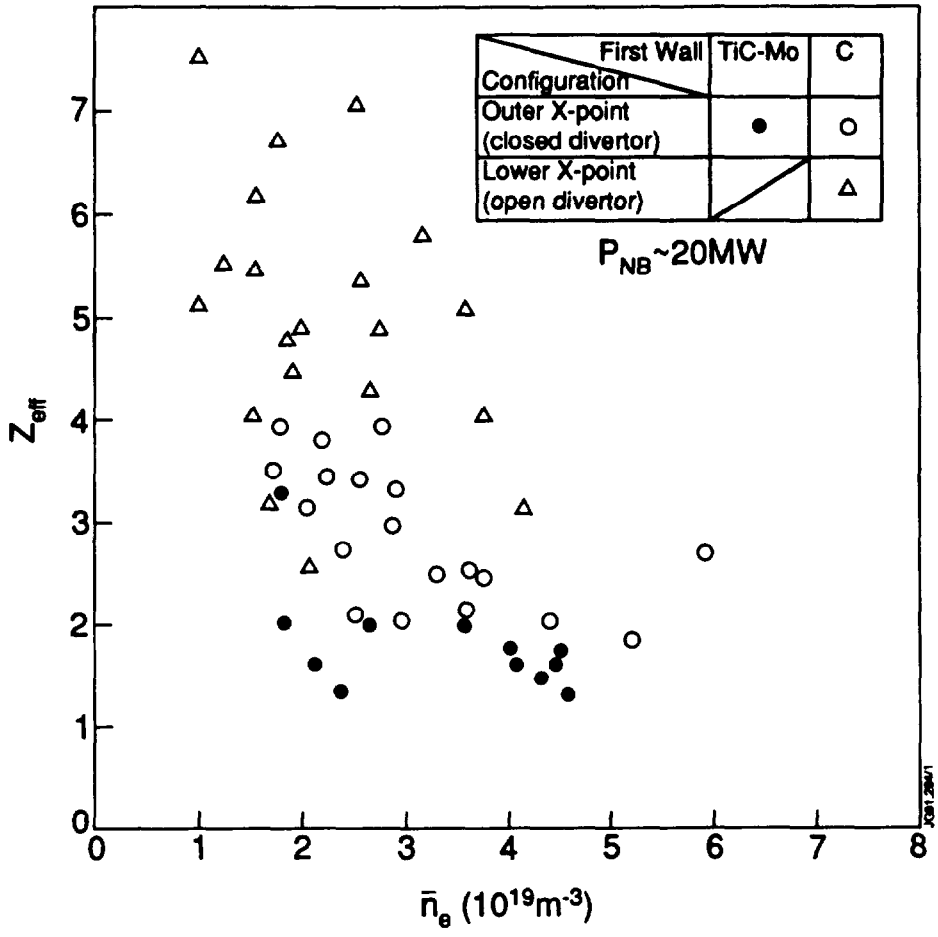

Fig. 1 Z_{eff} values in JT-60 beam heated discharges as a function of the line average density

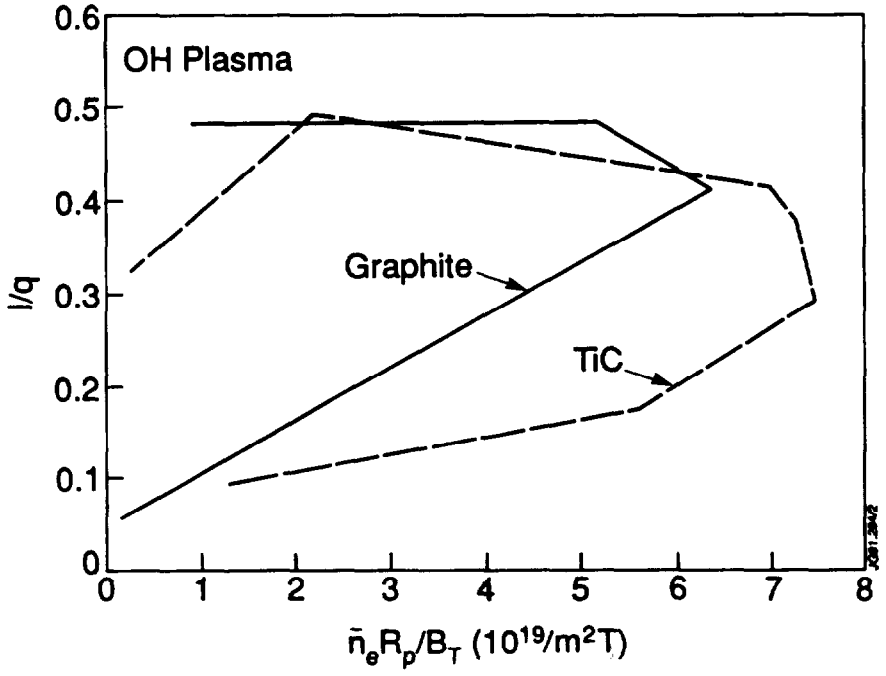

Fig. 2 Density limit with TiC and carbon walls in JT-60 for ohmic discharges

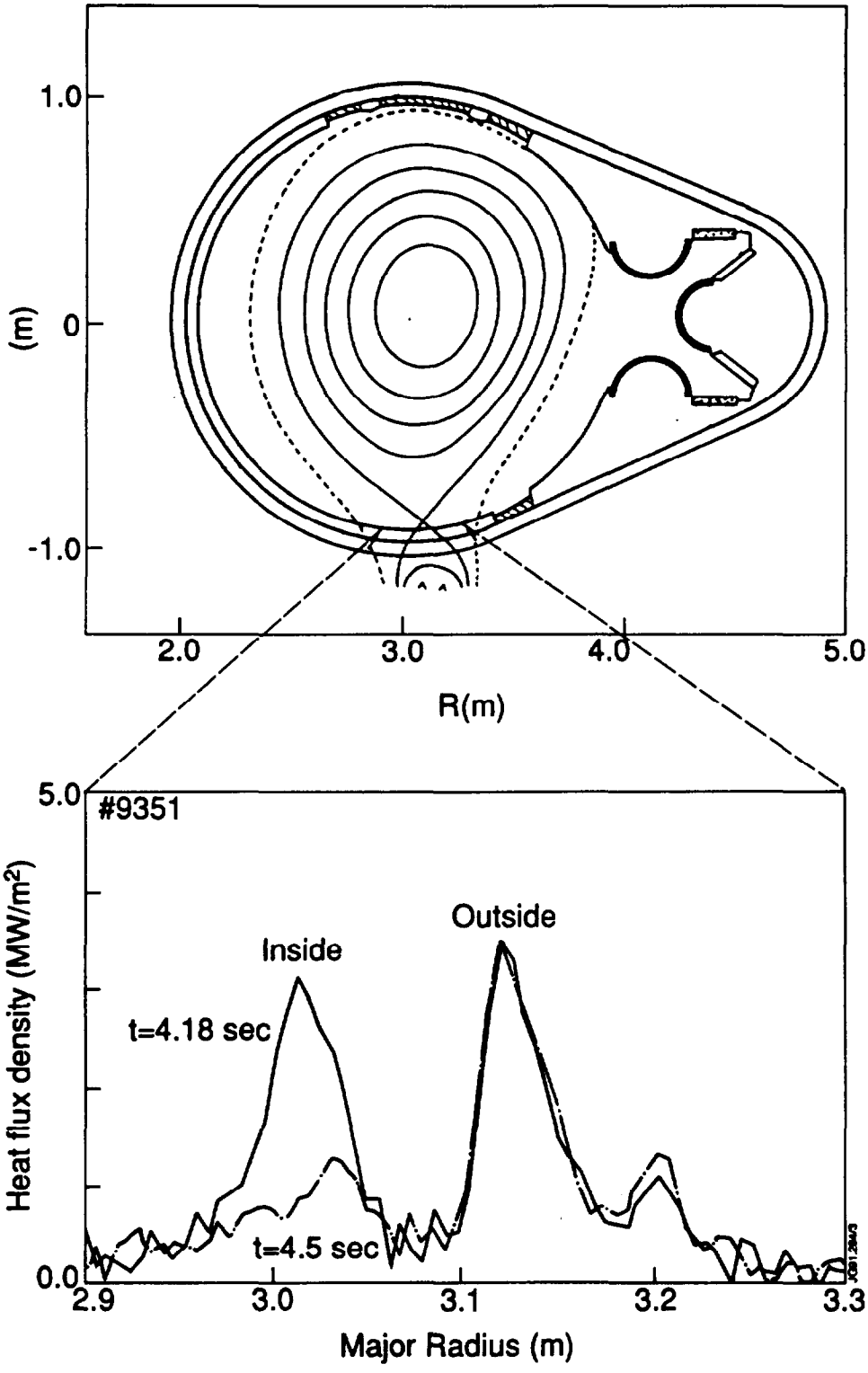

Fig. 3 Heat flux profiles in the divertor region of JT-60

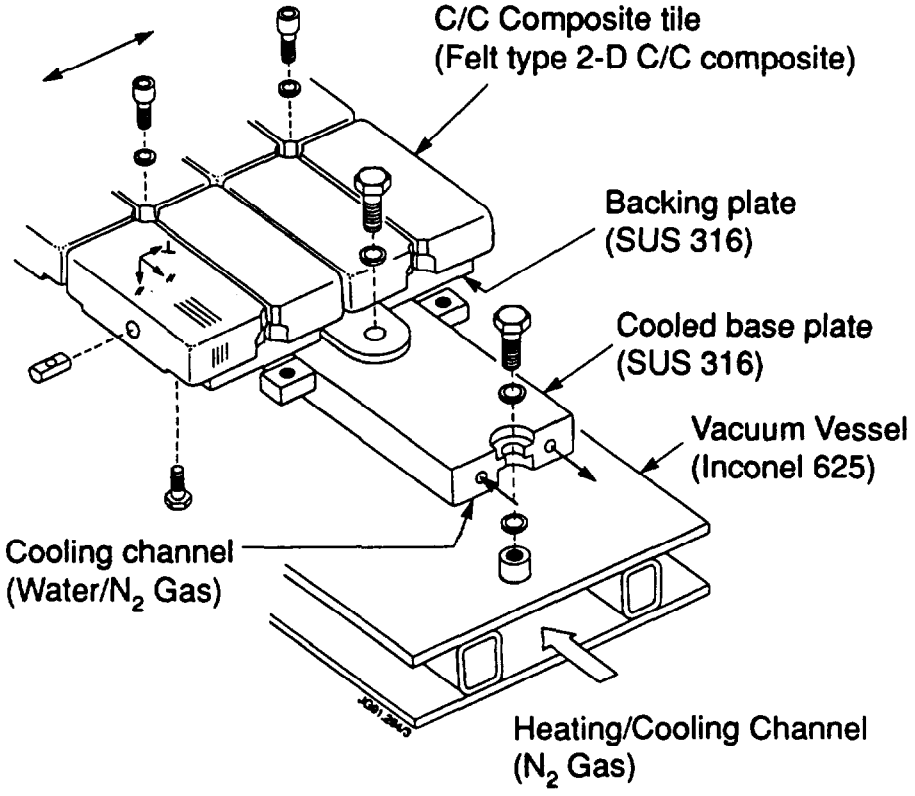

Fig. 4 Schematic of the divertor armour for JT-60

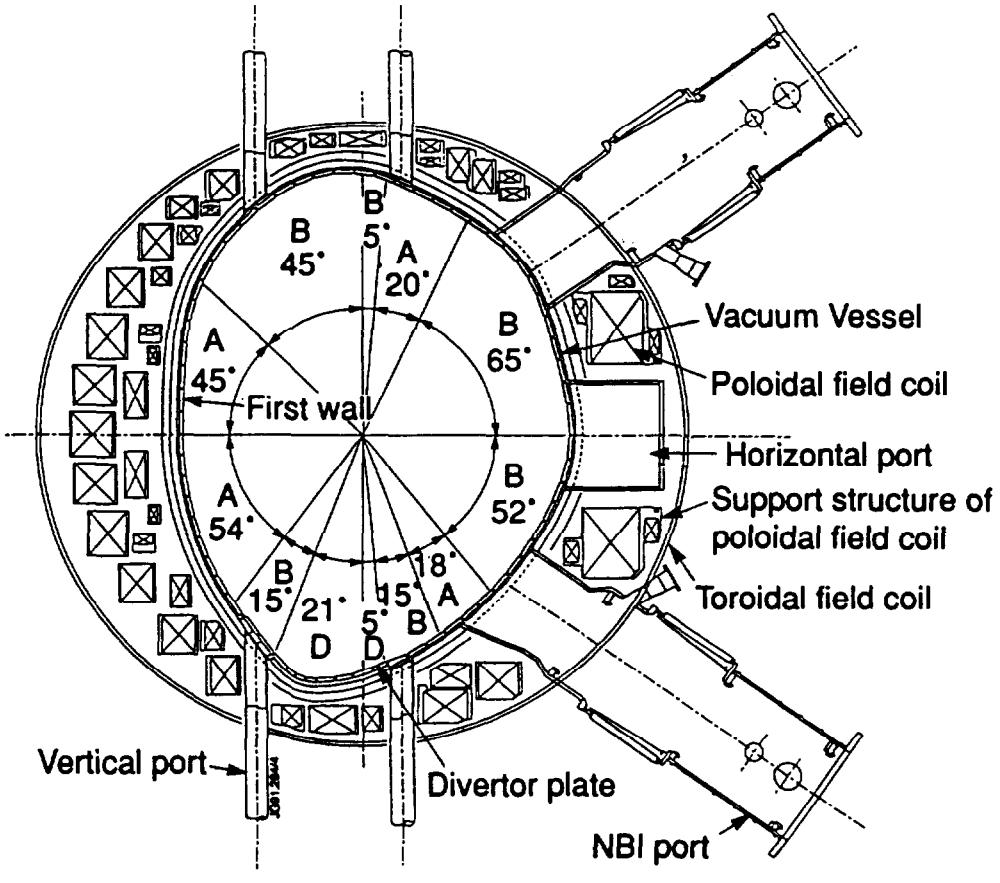

Fig. 5 Cross section through JT-60 Upgrade indicating regions for heat loads on first wall (A, B) and divertor (D)

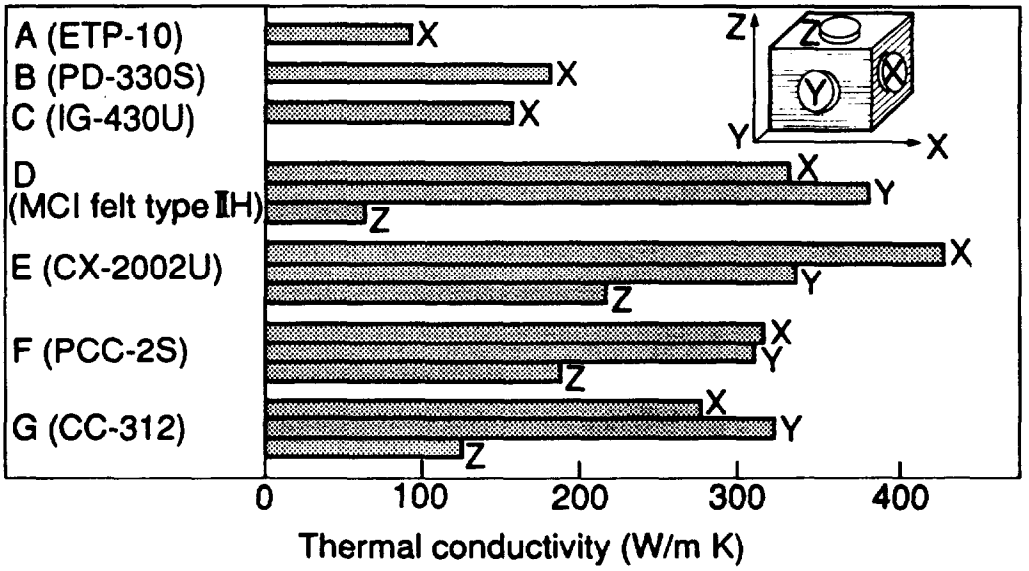

Fig. 6 Thermal conductivity of various carbon materials

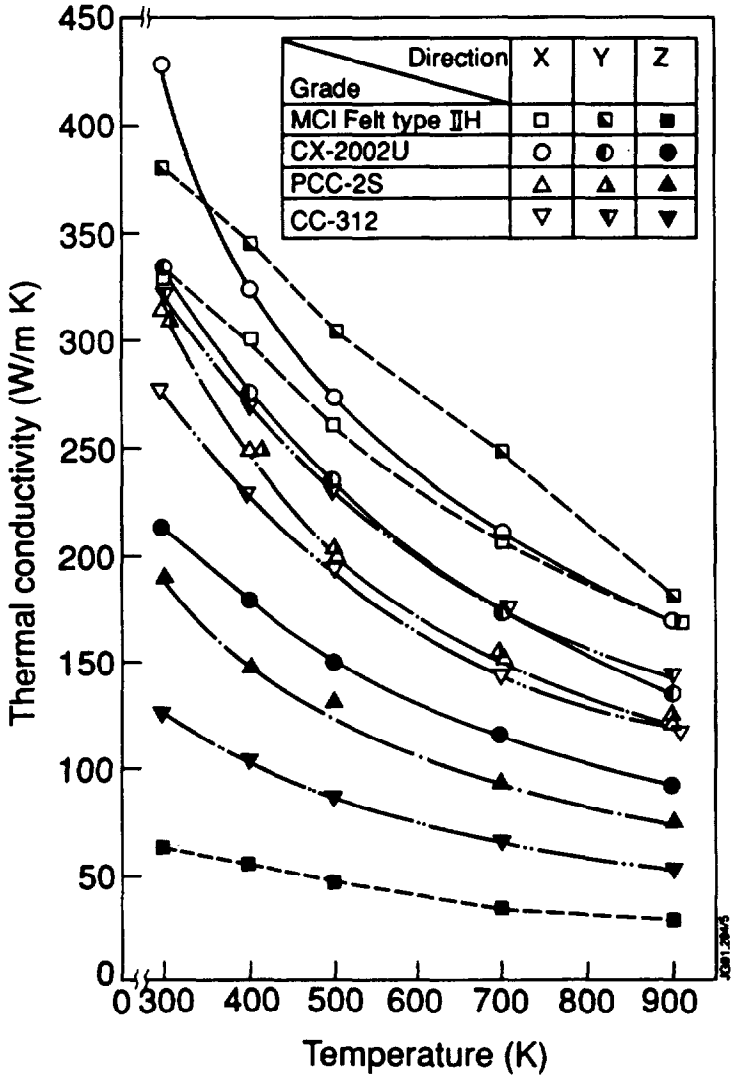

Fig. 7 Temperature dependence of thermal conductivity of carbon fibre composites

Fig. 8 Cross section of JT-60 Upgrade showing the wall armour

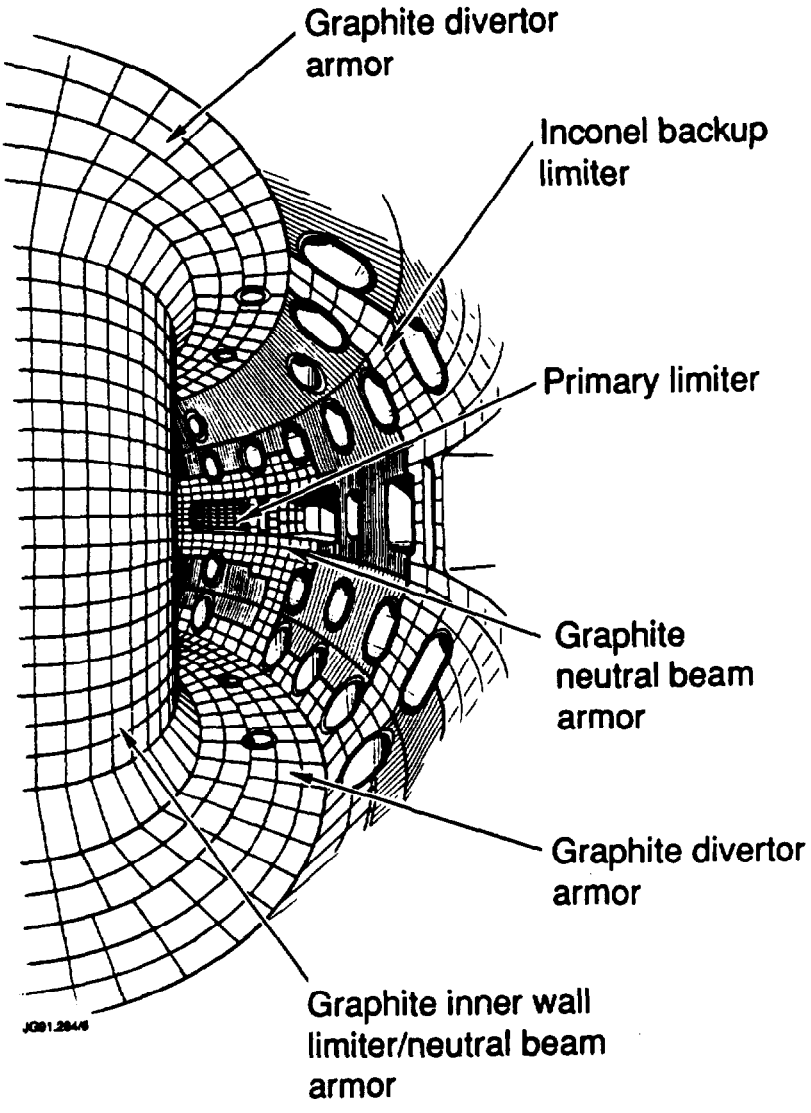

Fig. 9 The interior of the DIII-D tokamak and the location of the main high heat flux components. The divertor ring, installed in 1990, is not shown in this figure.

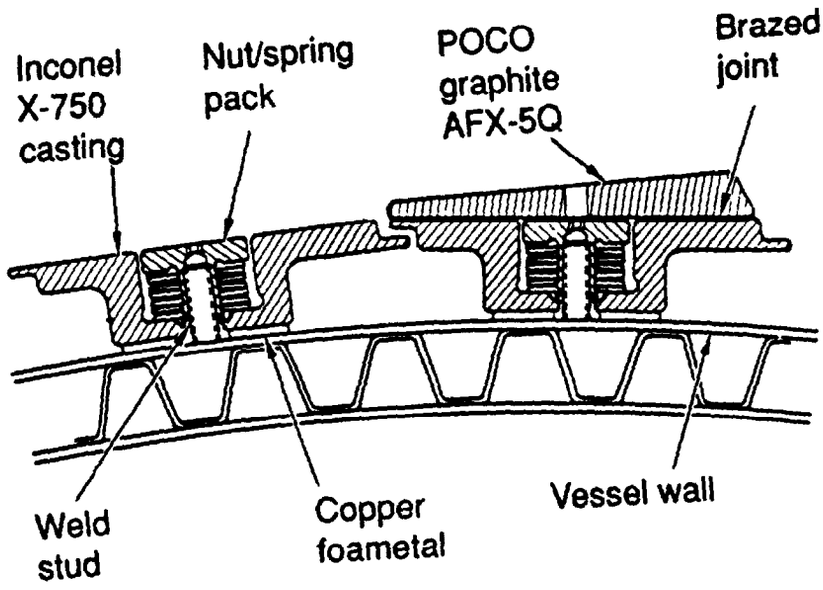

(a)

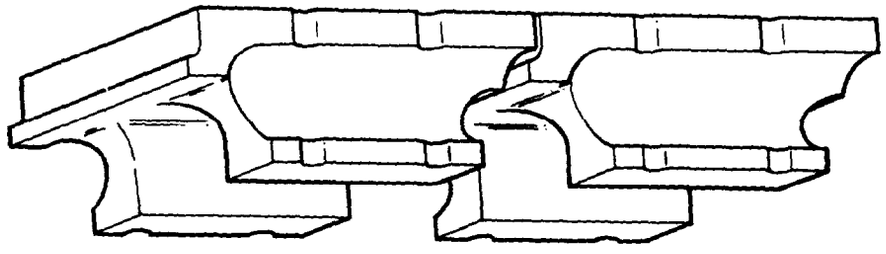

(b)

Fig. 10 Attachment of DIII-D graphite tiles to the vessel (a) and tile shaping (b)

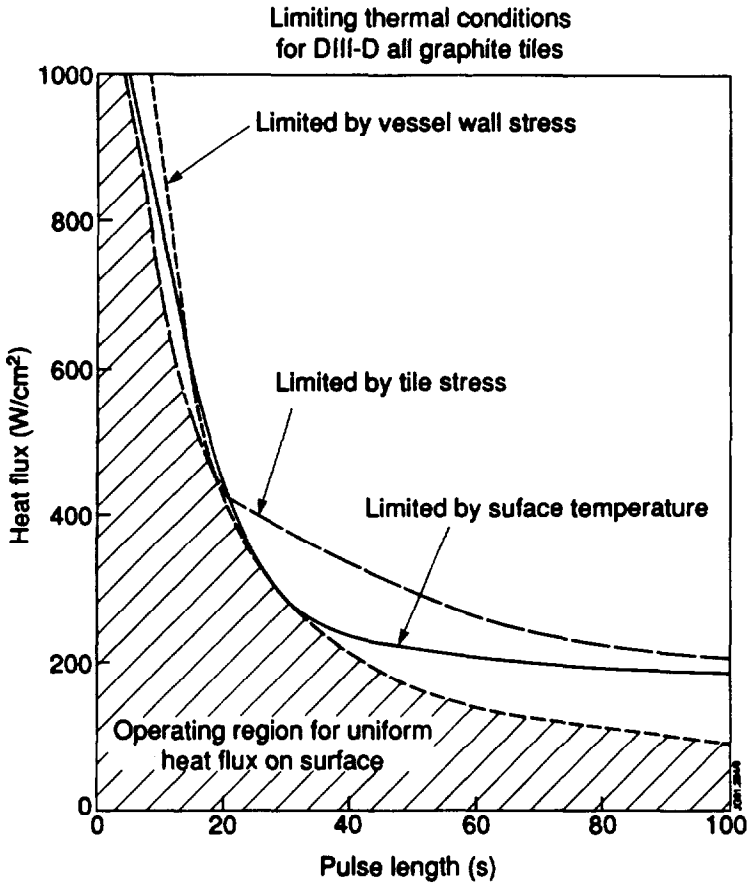

Fig.11 Thermal limits for the DIII-D graphite tiles assuming a constant heat flux over the plasma facing surface of the tile (from [14]).

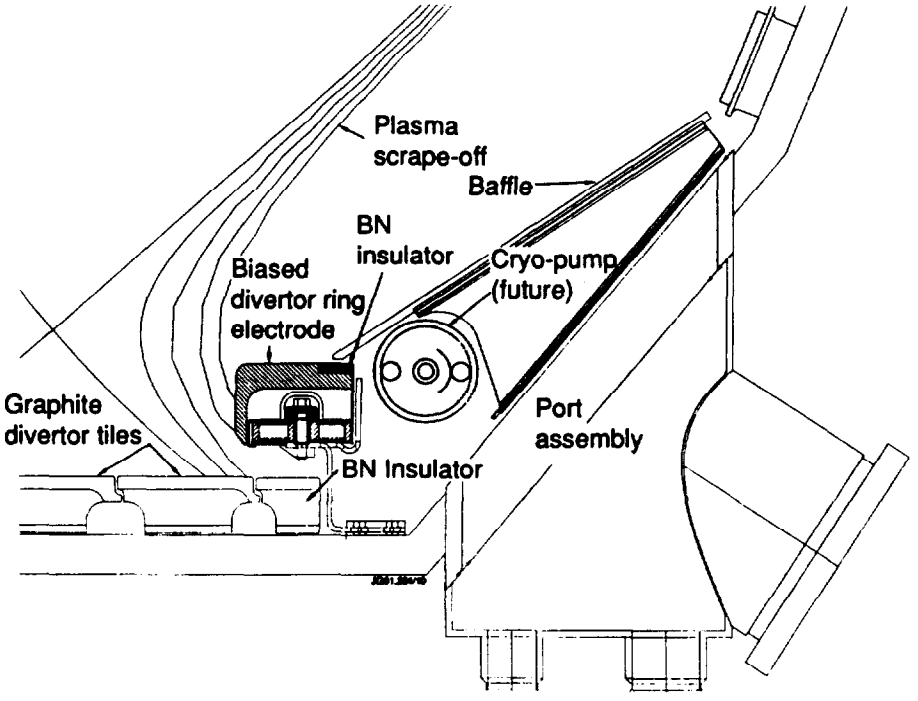

Fig. 12 Schematic of the divertor ring installed in the lower outside region of DIII-D (see Fig. 9). The flux surfaces which define the plasma boundary and scrape-off region are shown for a 'typical' tokamak discharge.

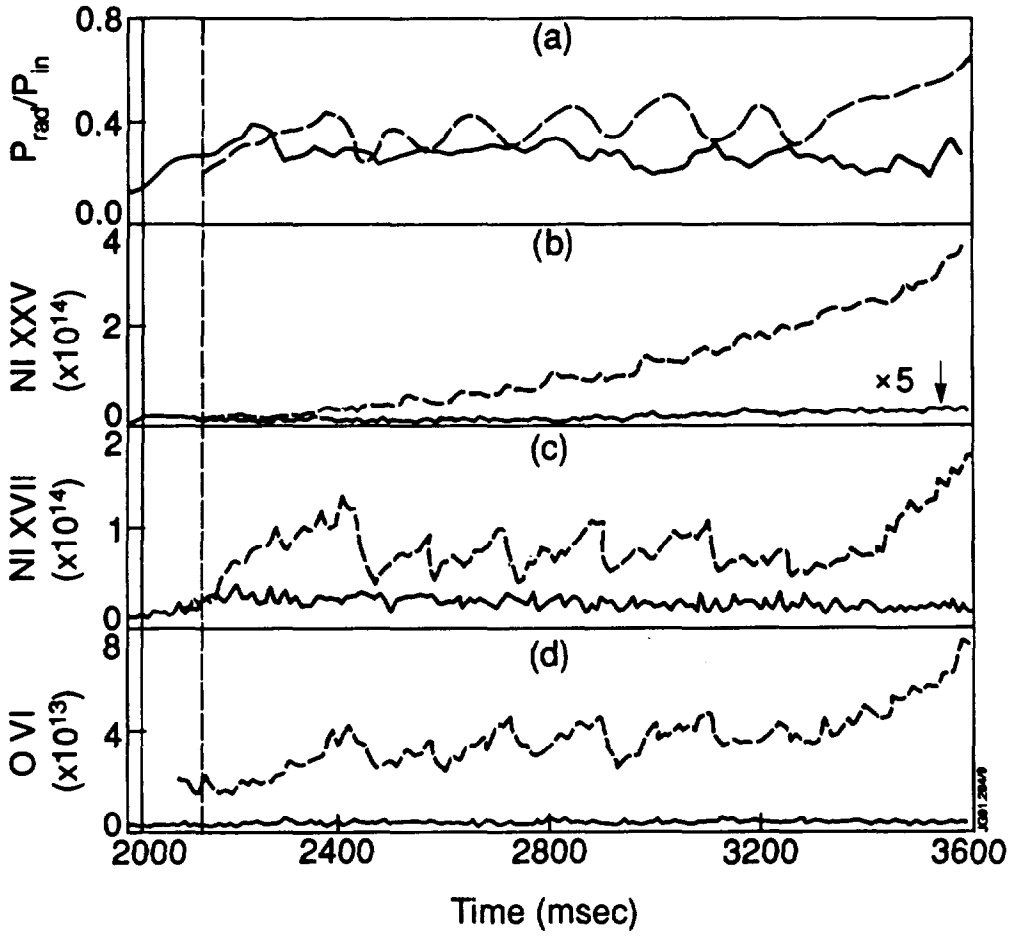

Fig. 13 Impurity behaviour in DIII-D before (dashed line) and after (solid line) carbonisation. The transition time for L-mode to H-mode is shown as a vertical line for both discharges (from [18]). Discharge conditions are I_p = 2 MA, B_t = 2.1 T, and P_{NBI} = 6.5 MW

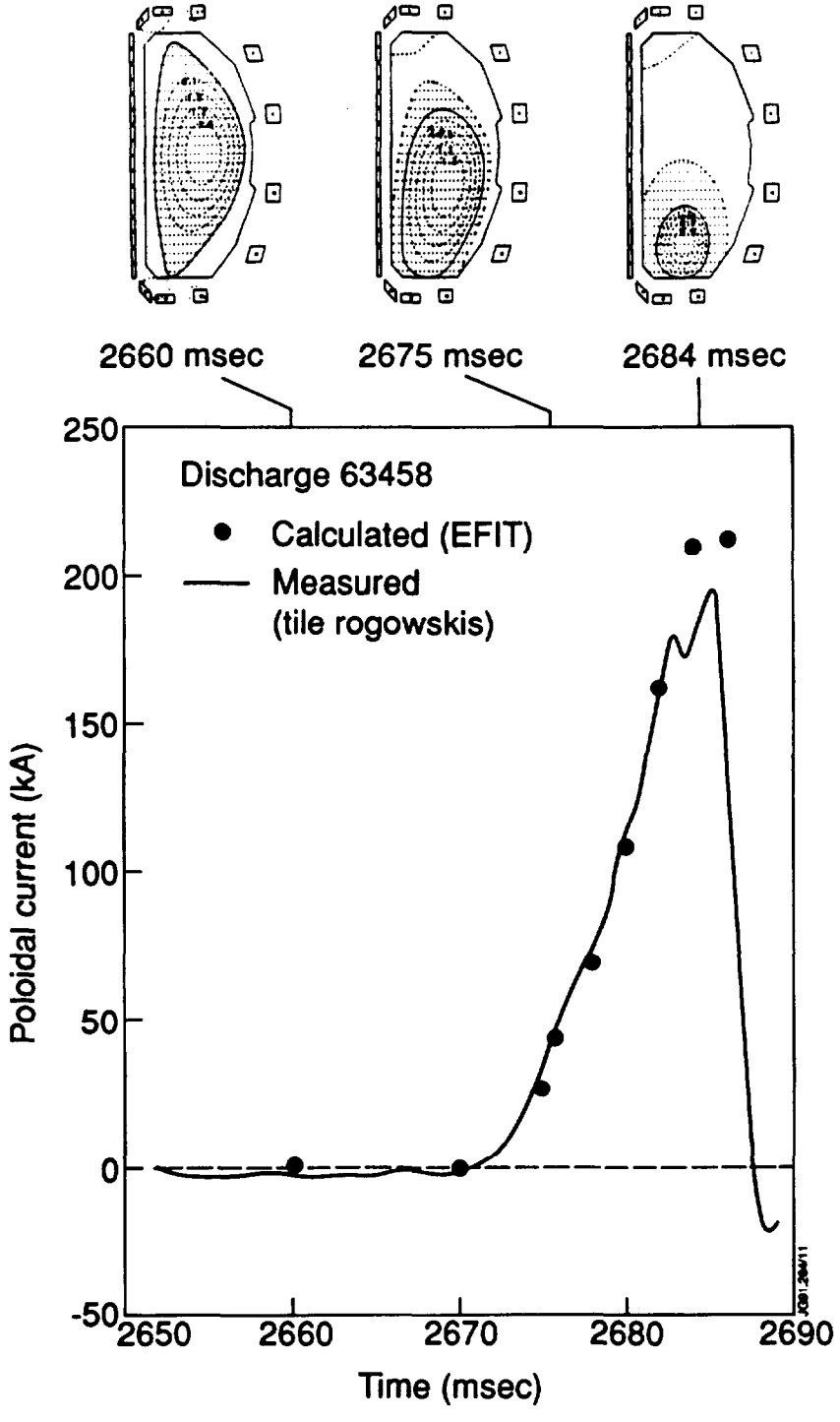

Fig. 14 Measured and calculated poloidal tile current in DIII-D during a disruption as a function of time, I_p = 1 MA (from [18])

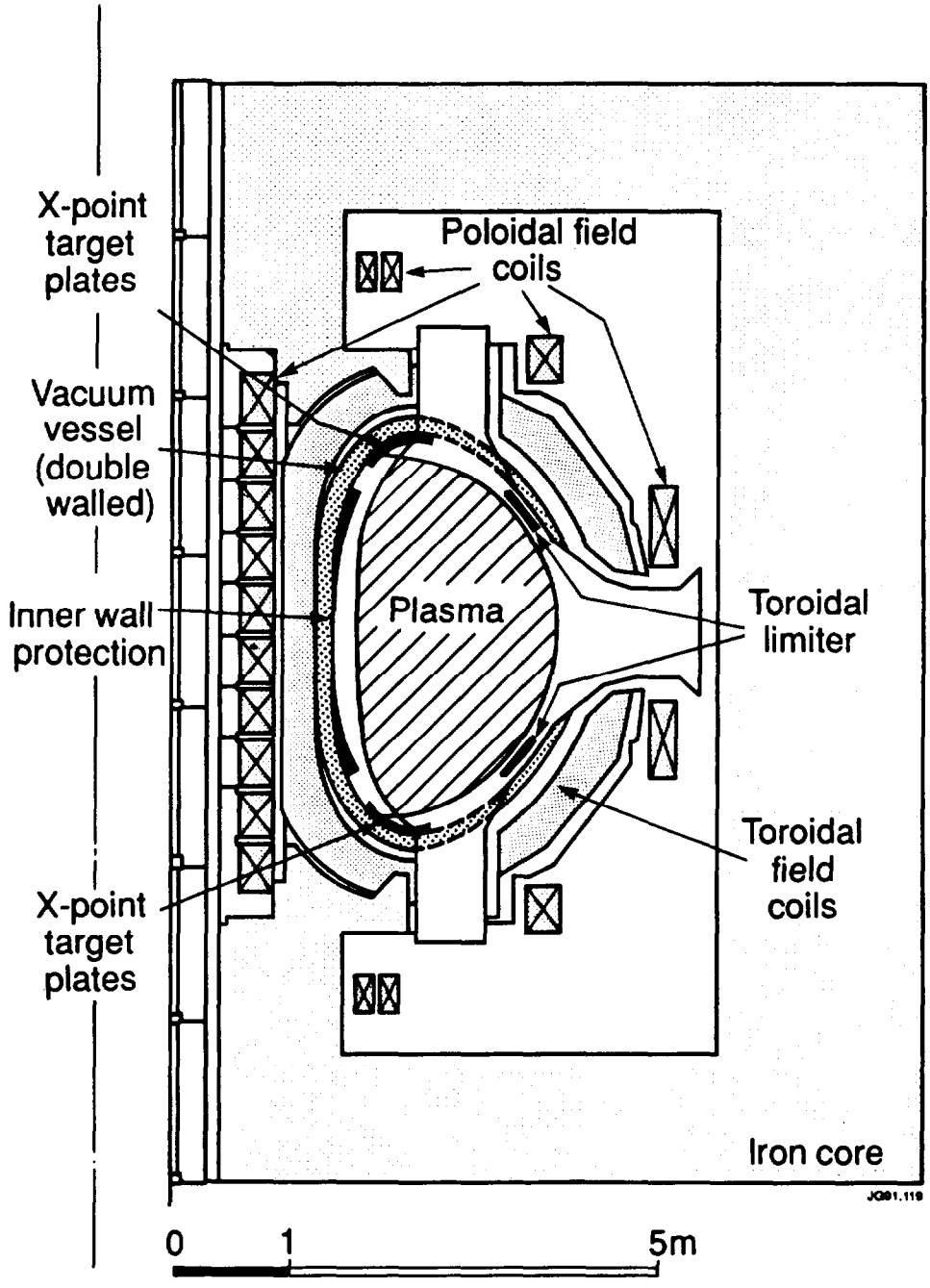

Fig. 15 Schematic cross-section through JET showing in vessel components

Fig. 16 Example of inner wall damage due to halo currents in JET

Table 1

Typical impurity concentrations and radiation losses in JT-60 for divertor (outer X-point and closed configuration) and limiter operation. The subscripts e, C, Ti and O denote electrons, carbon, titanium and oxygen.

First Wall	Metallic Wall (TiC-Mo)		Graphite Wall	
Configuration	Divertor	Limiter	Divertor	Limiter
Z_{eff}	1.6	---	2.2	3-5
n_C/n_e (%)	0.2	---	0.8	4-9
n_O/n_e (%)	1	---	2	1-2
n_{Ti}/n_e (%)	0.006	---	$5X10^{-4}$ - $2x10^{-3}$	---
Radiation Loss (%) (Main Plasma)	10	> 60	15	20

Table 2

Impurity content (%) and dilution (on axis density ratio of deuterons to electrons) for typical JET discharges with different wall materials

	C Phase	Be/C Phase	Be Phase	
	Limiter	Limiter	Limiter	X-point
Oxygen (%)	1	0.05	0.05	0.05
Carbon (%)	5	3	0.5	1.5
Beryllium (%)	---	1	3	1
Dilution (n_D/n_e)	0.6	0.8	0.85	0.9

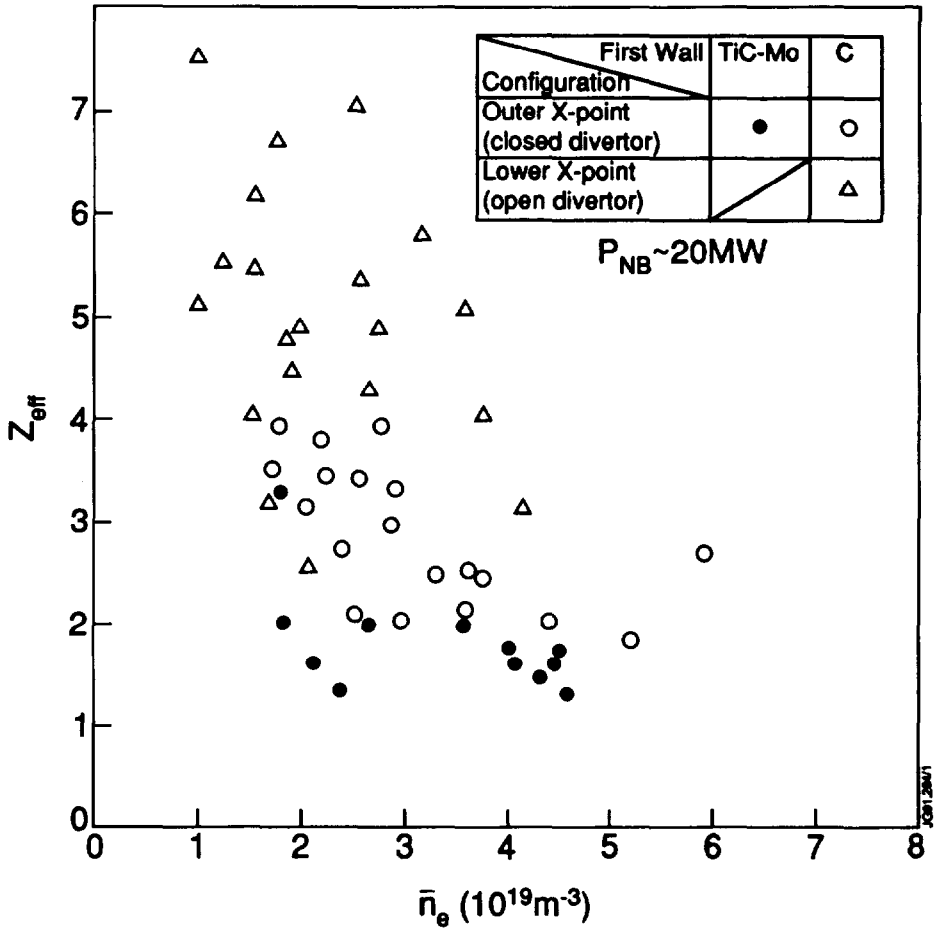

Fig. 1 Z_{eff} values in JT-60 beam heated discharges as a function of the line average density

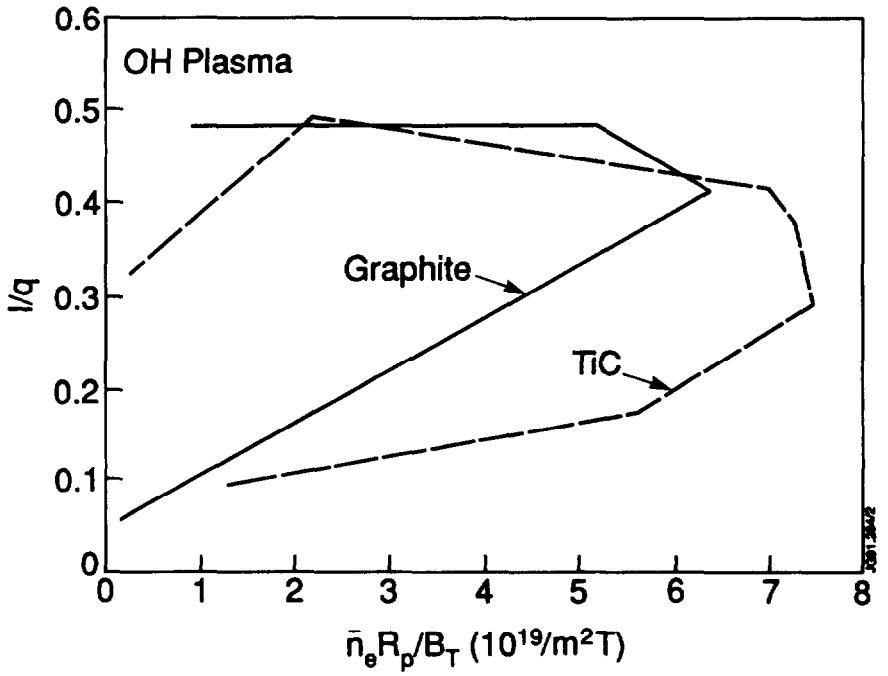

Fig. 2 Density limit with TiC and carbon walls in JT-60 for ohmic discharges

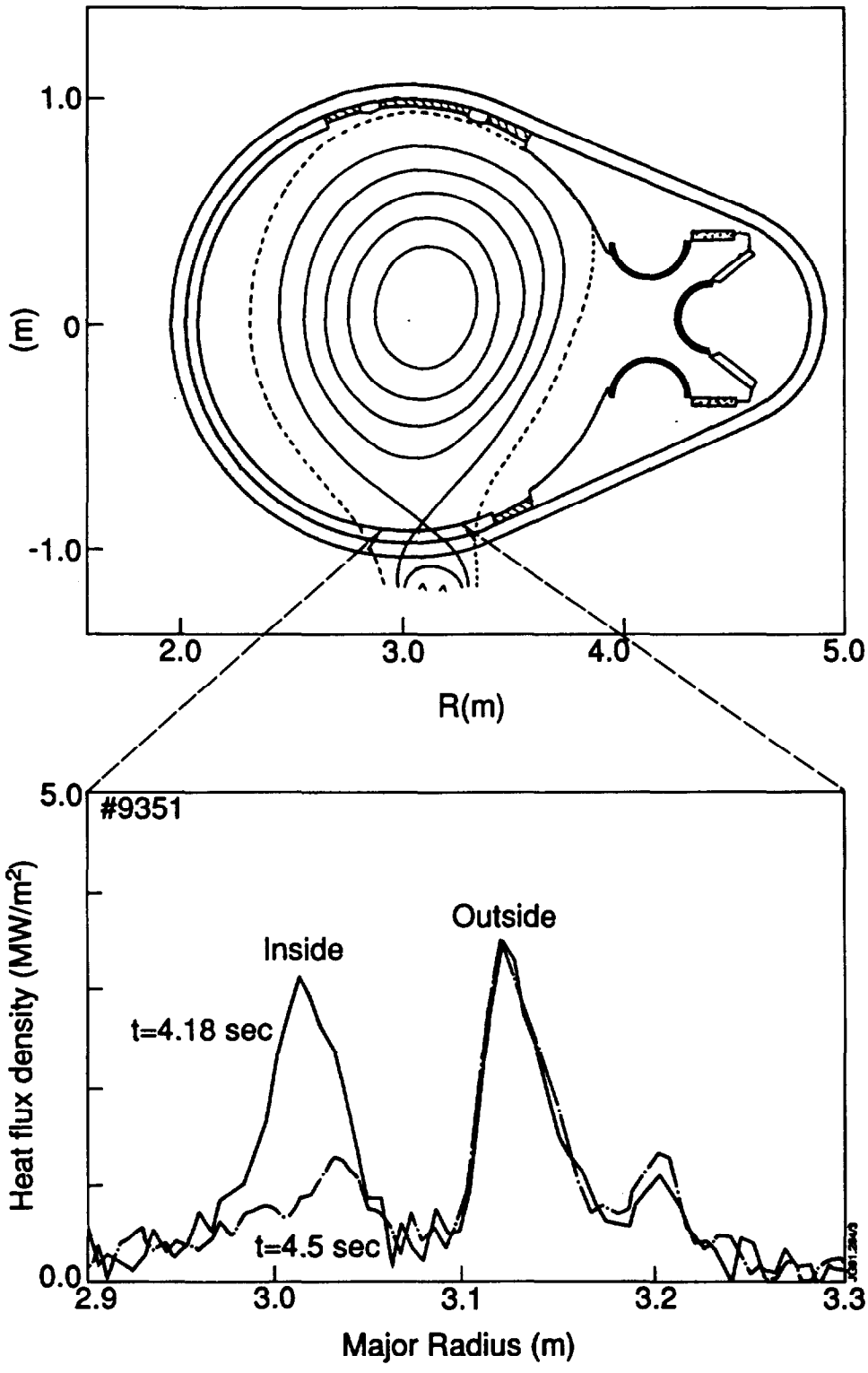

Fig. 3 Heat flux profiles in the divertor region of JT-60

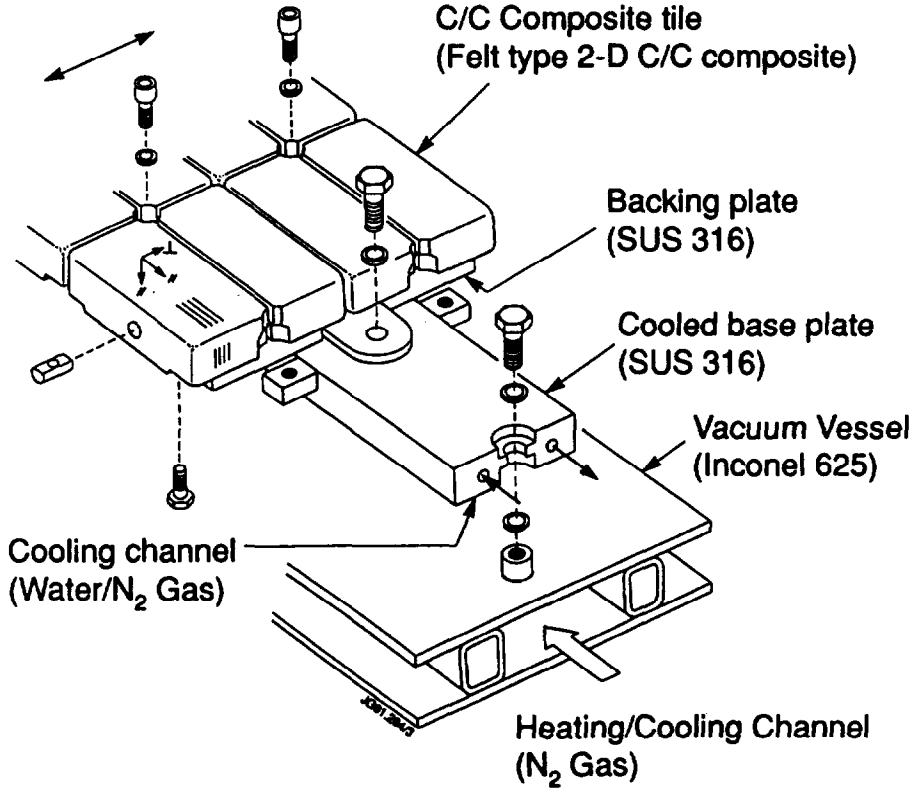

Fig. 4 Schematic of the divertor armour for JT-60

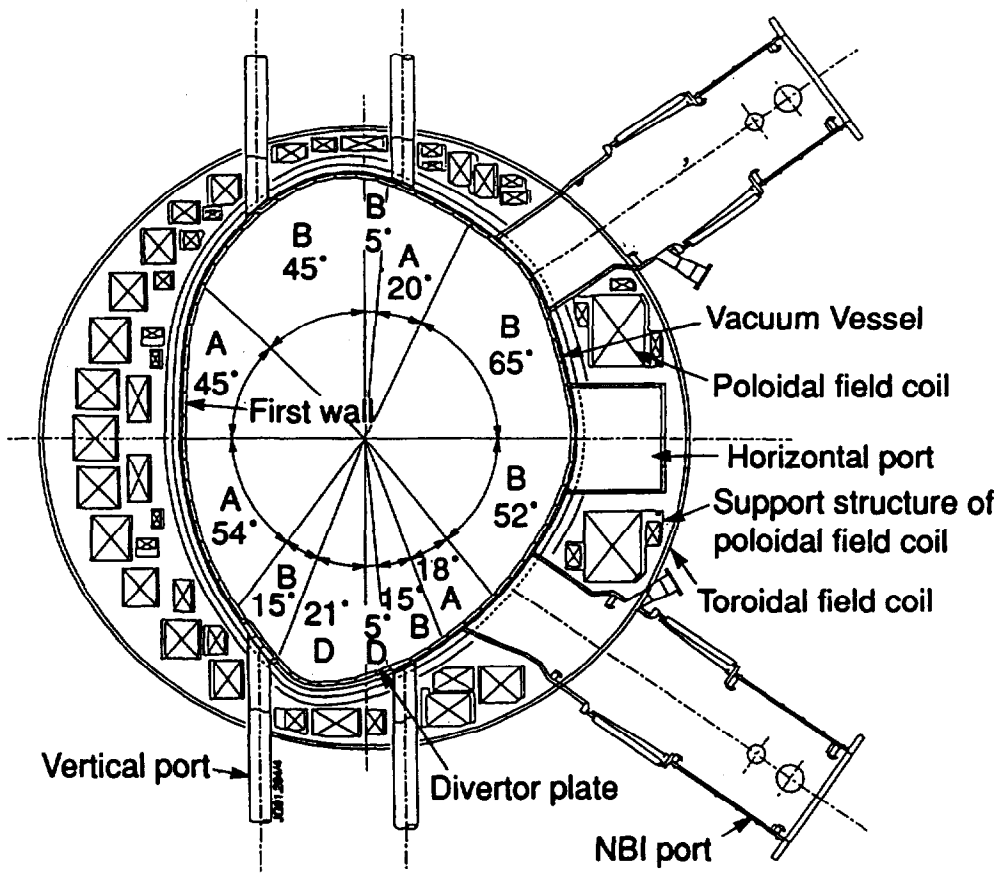

Fig. 5 Cross section through JT-60 Upgrade indicating regions for heat loads on first wall (A, B) and divertor (D)

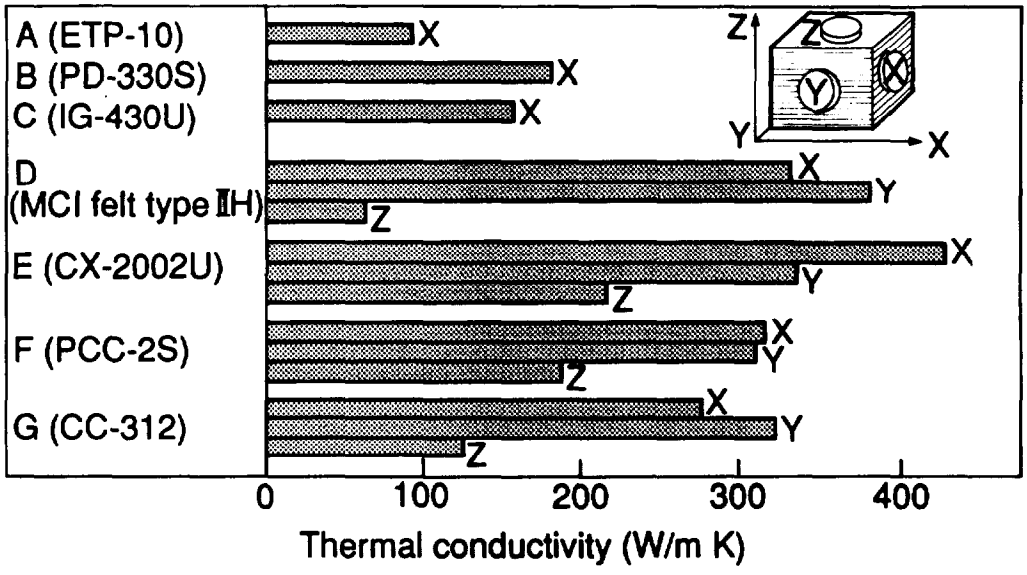

Fig. 6 Thermal conductivity of various carbon materials

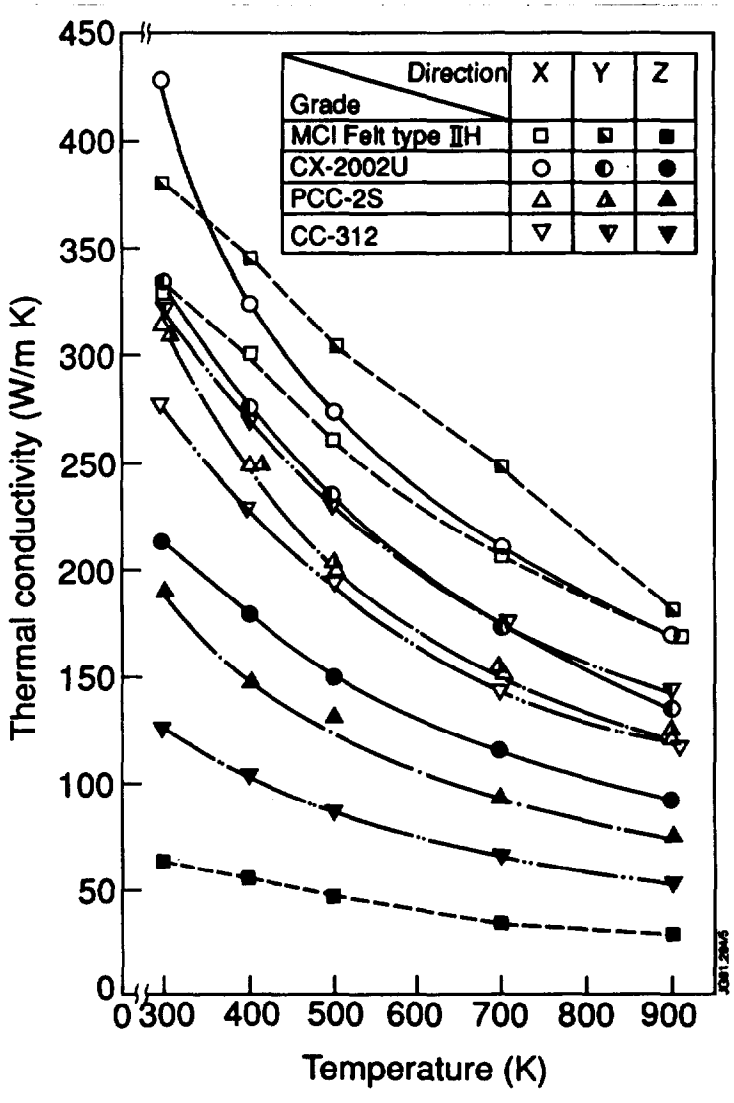

Fig. 7 Temperature dependence of thermal conductivity of carbon fibre composites

Fig. 8 Cross section of JT-60 Upgrade showing the wall armour

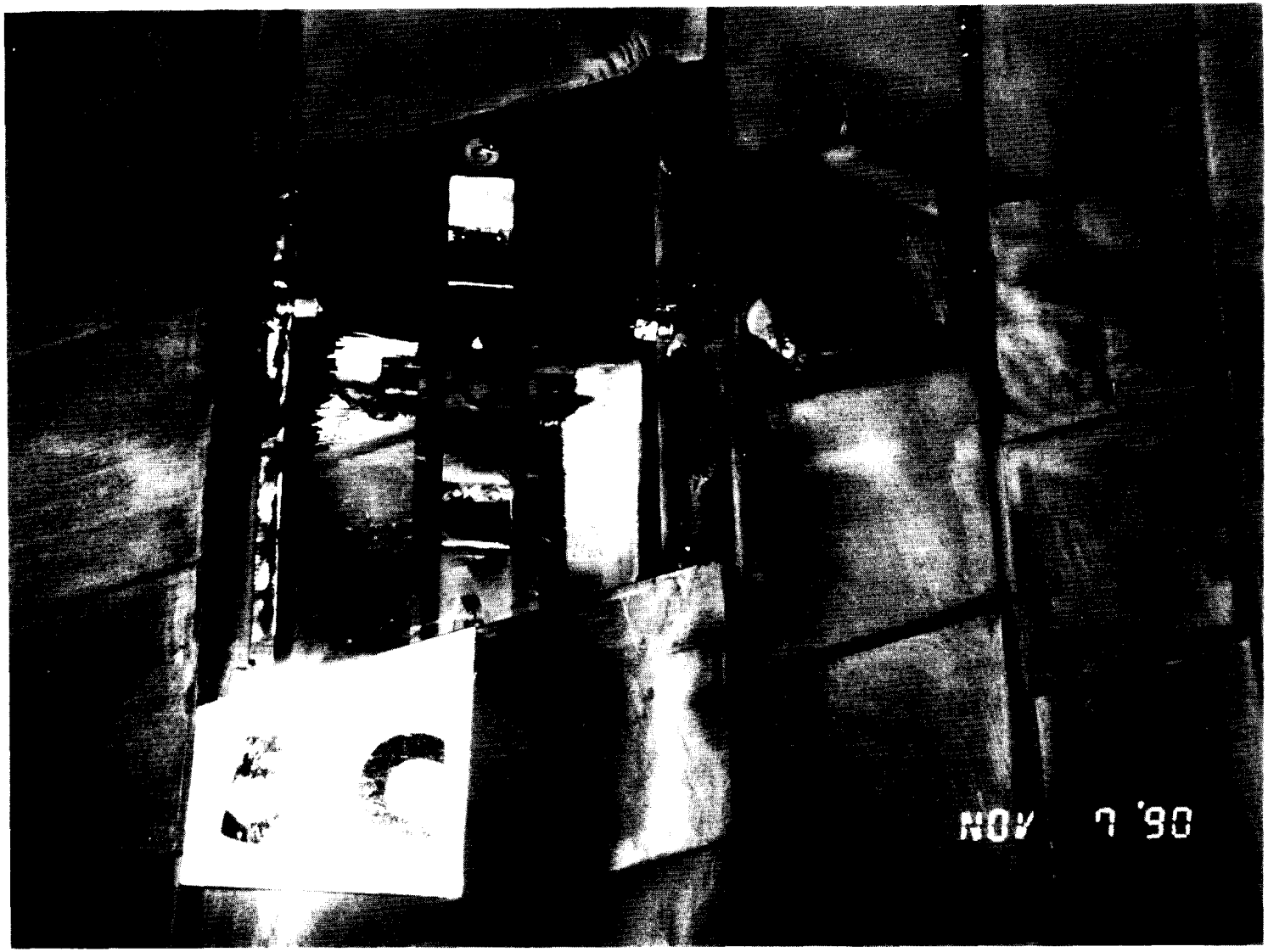

Fig. 16 Example of inner wall damage due to halo currents in JET

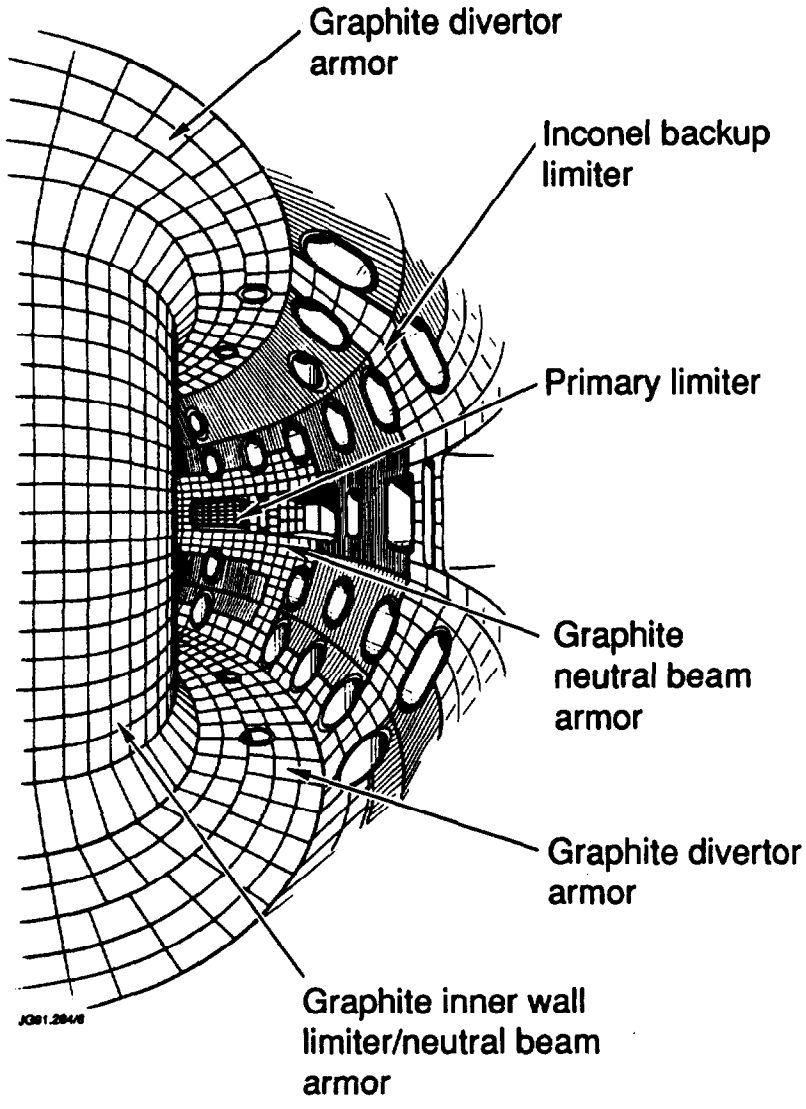

Fig. 9 The interior of the DIII-D tokamak and the location of the main high heat flux components. The divertor ring, installed in 1990, is not shown in this figure.

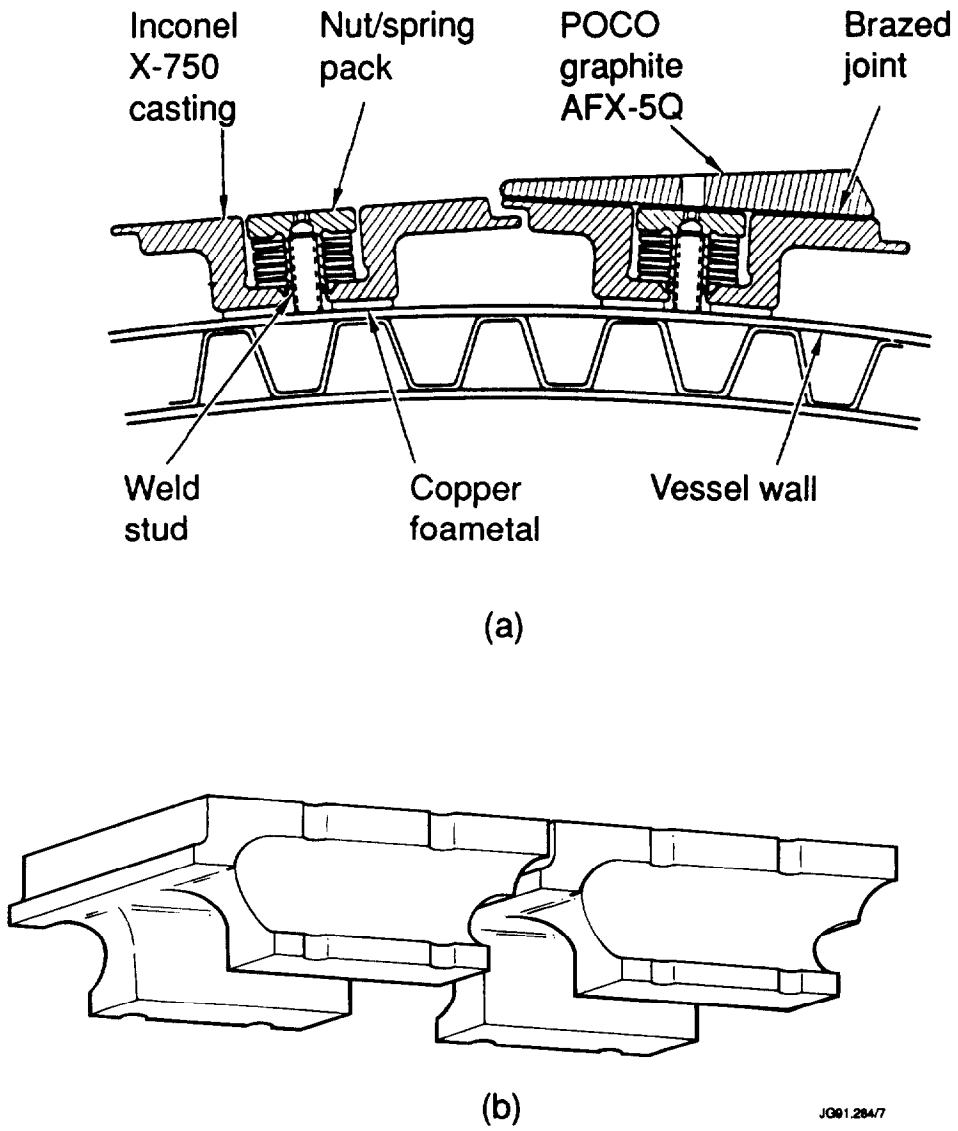

Fig. 10 Attachment of DIII-D graphite tiles to the vessel (a) and tile shaping (b)

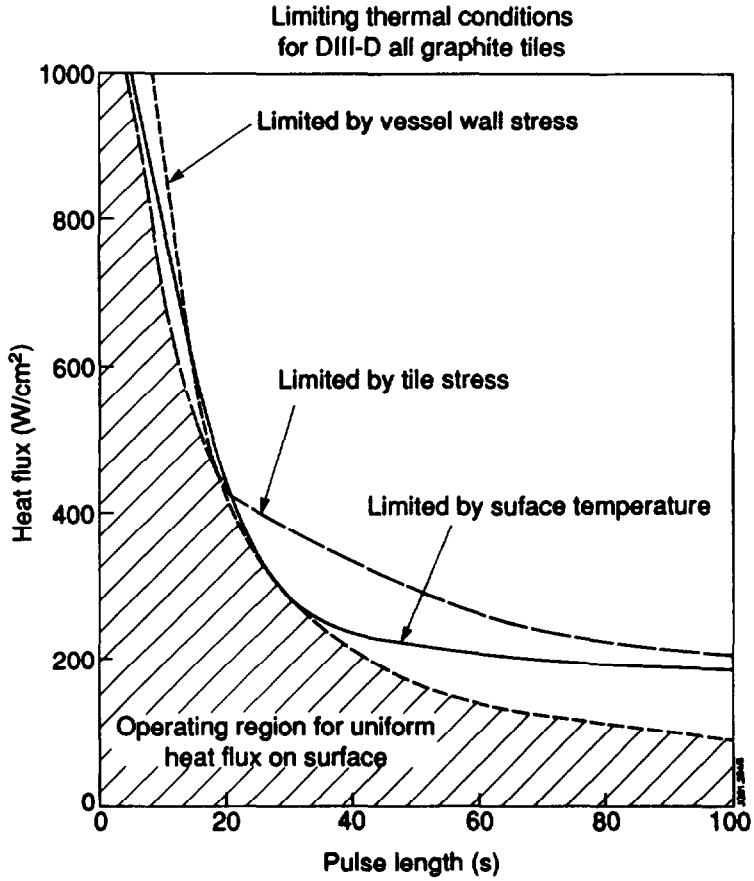

Fig.11 Thermal limits for the DIII-D graphite tiles assuming a constant heat flux over the plasma facing surface of the tile (from [14]).

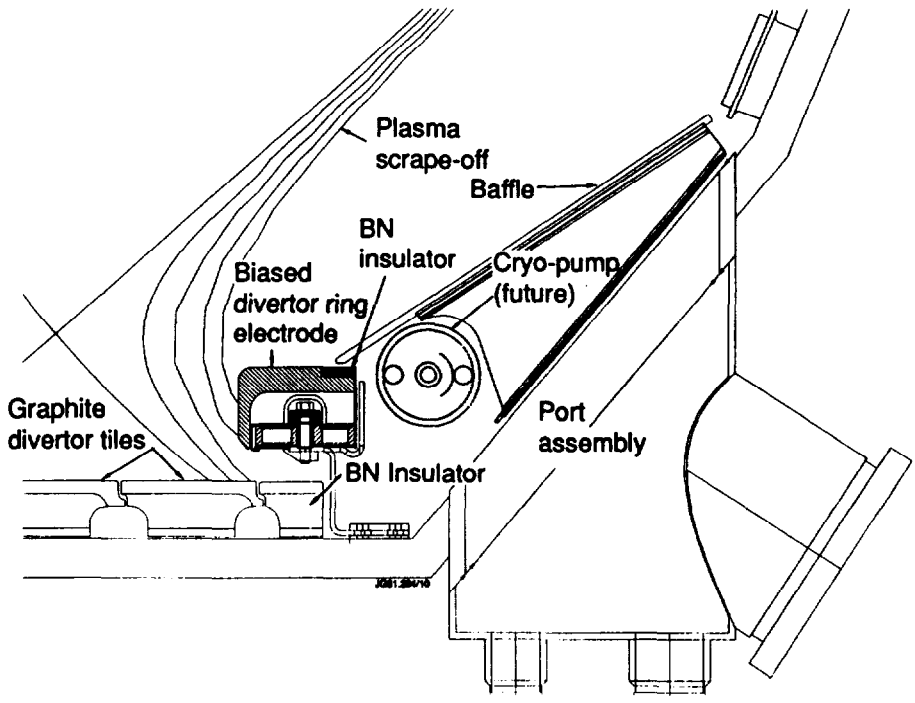

Fig. 12 Schematic of the divertor ring installed in the lower outside region of DIII-D (see Fig. 9). The flux surfaces which define the plasma boundary and scrape-off region are shown for a 'typical' tokamak discharge.

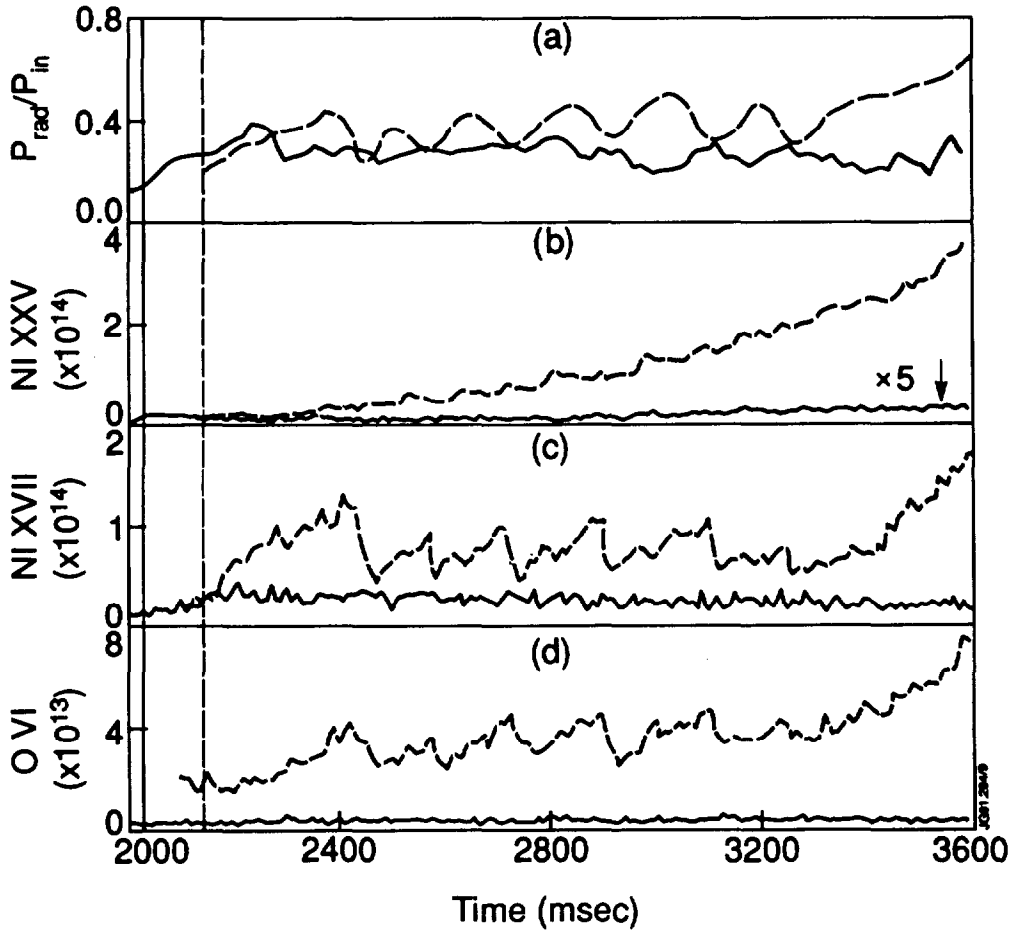

Fig. 13 Impurity behaviour in DIII-D before (dashed line) and after (solid line) carbonisation. The transition time for L-mode to H-mode is shown as a vertical line for both discharges (from [18]). Discharge conditions are I_p = 2 MA, B_t = 2.1 T, and P_{NBI} = 6.5 MW

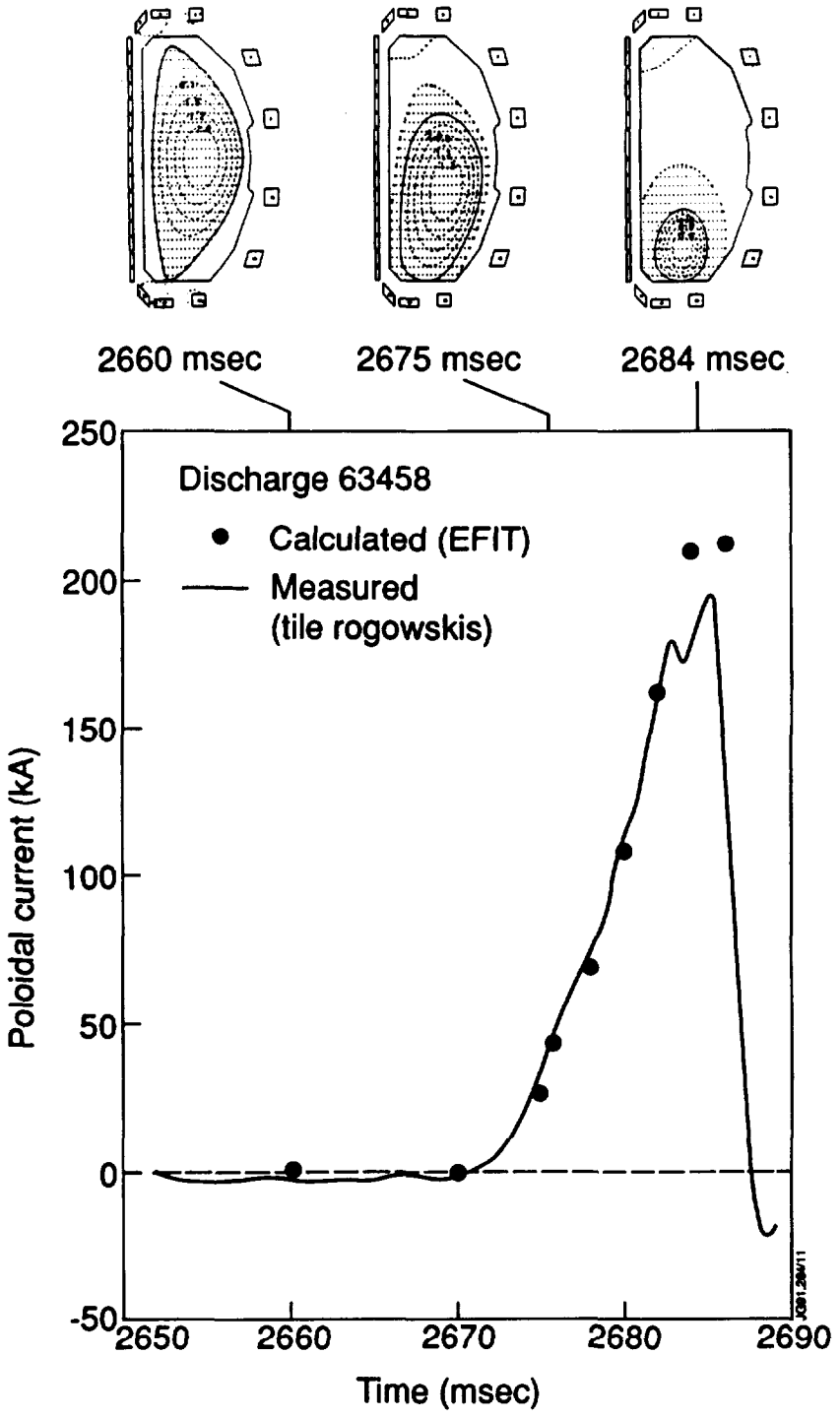

Fig. 14 Measured and calculated poloidal tile current in DIII-D during a disruption as a function of time, I_p = 1 MA (from [18])

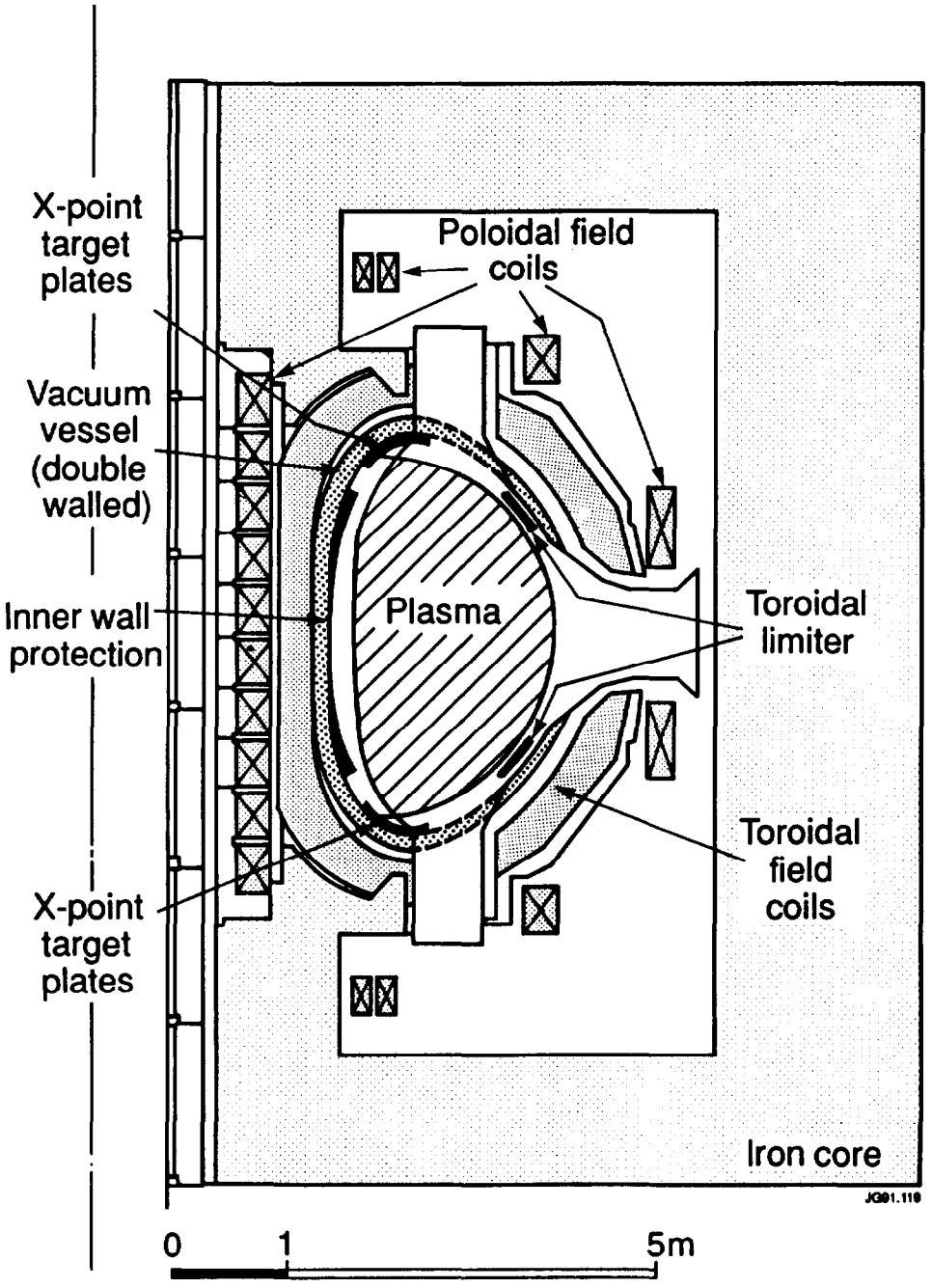

Fig. 15 Schematic cross-section through JET showing in vessel components

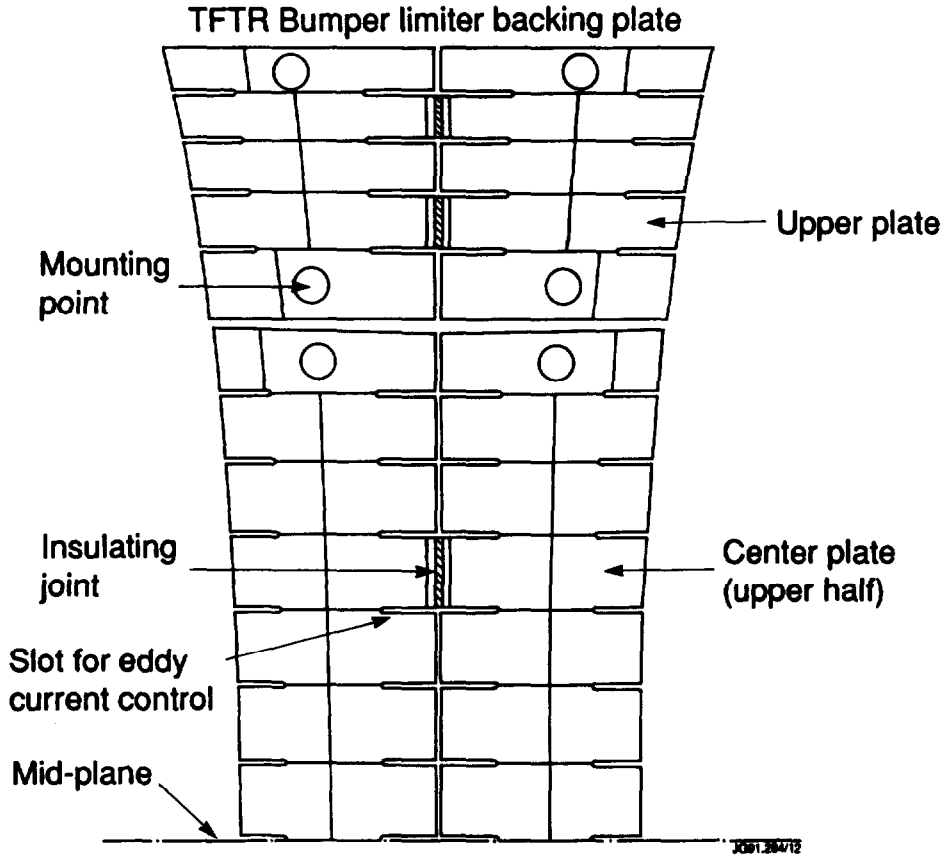

Fig. 18 TFR Bumper Limiter backing plate

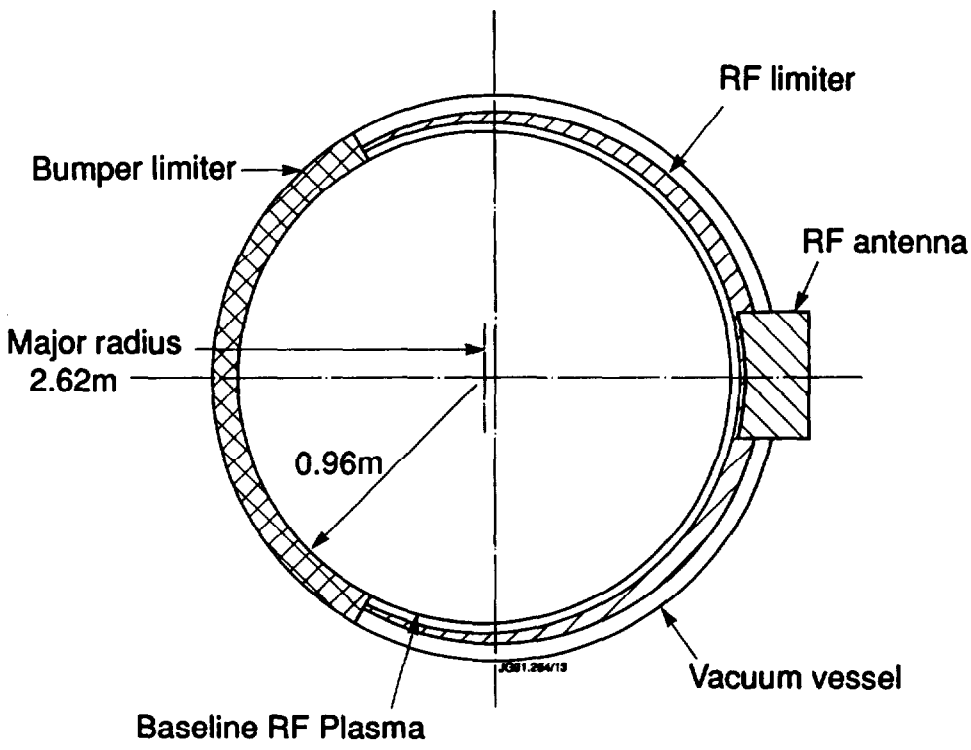

Fig. 19 Cross-Section of TFTR showing Bumper Limiter, RF antenna and limiter

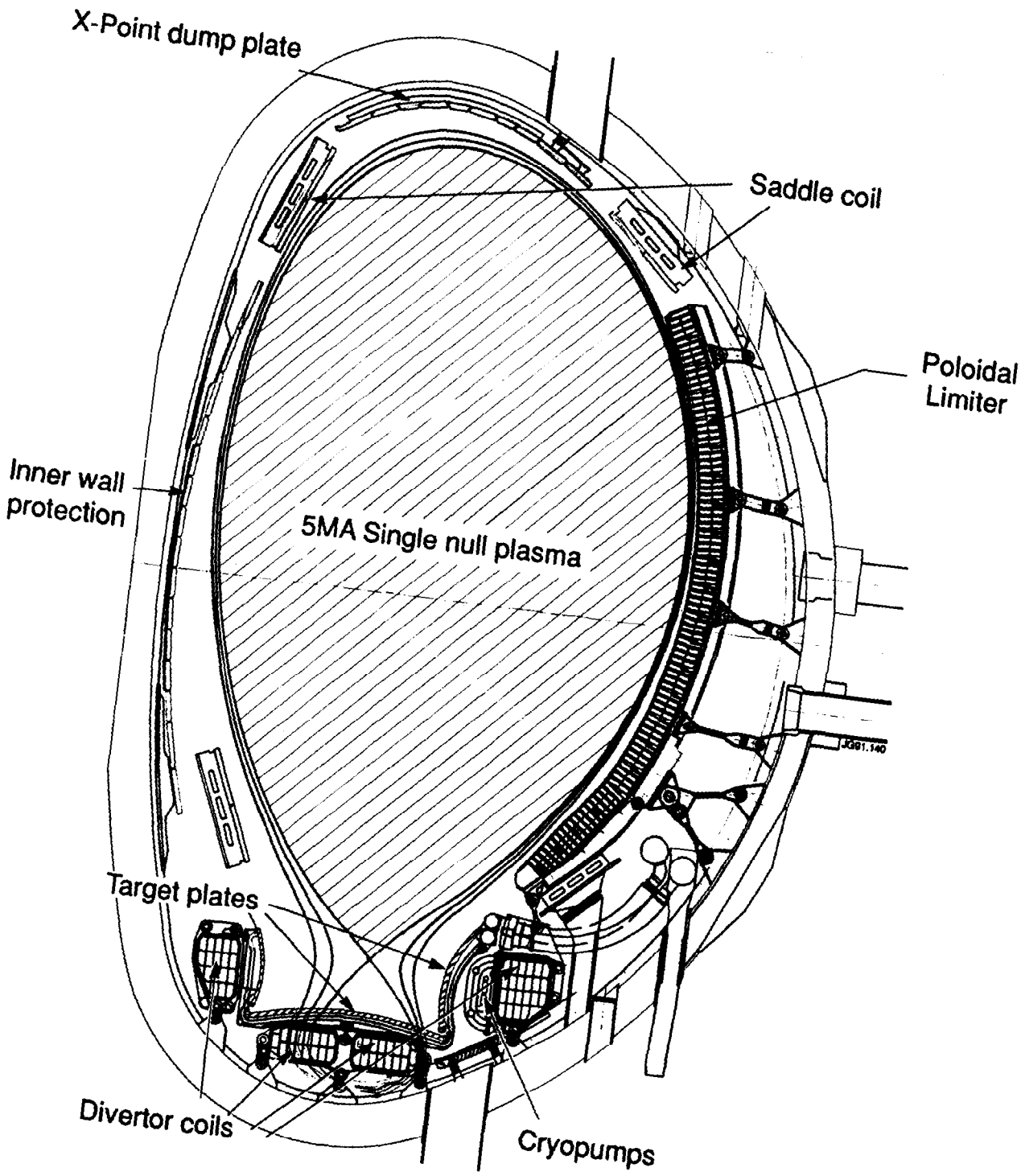

Fig. 17 JET Pumped Divertor configuration for a 5 MA Single Null plasma

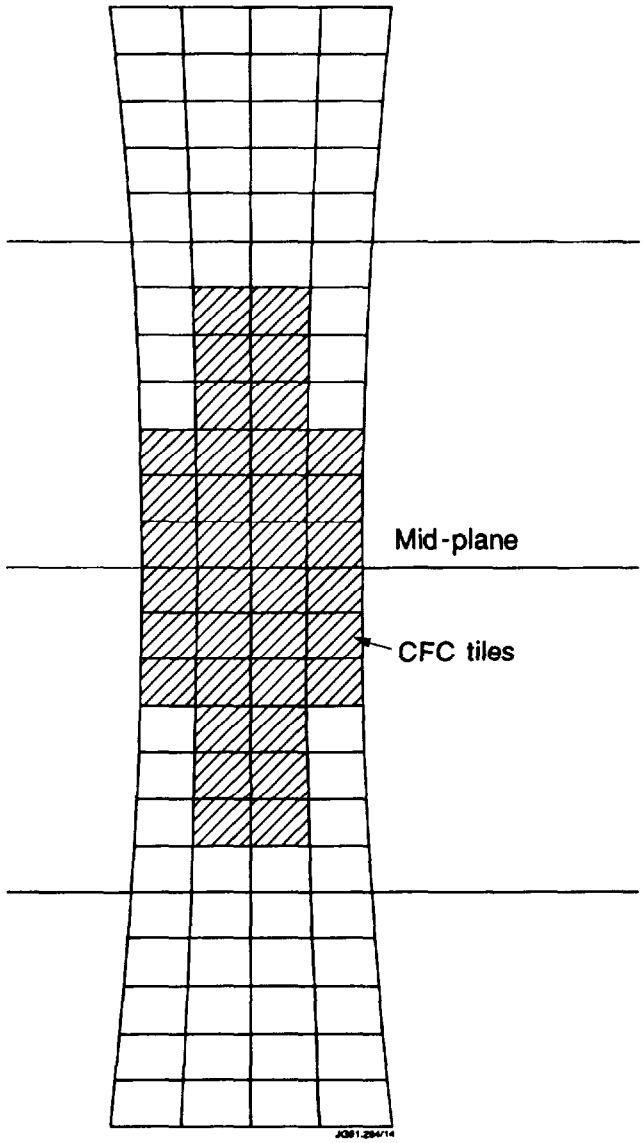

Fig. 20 Areas of the Bumper Limiter covered with CFC

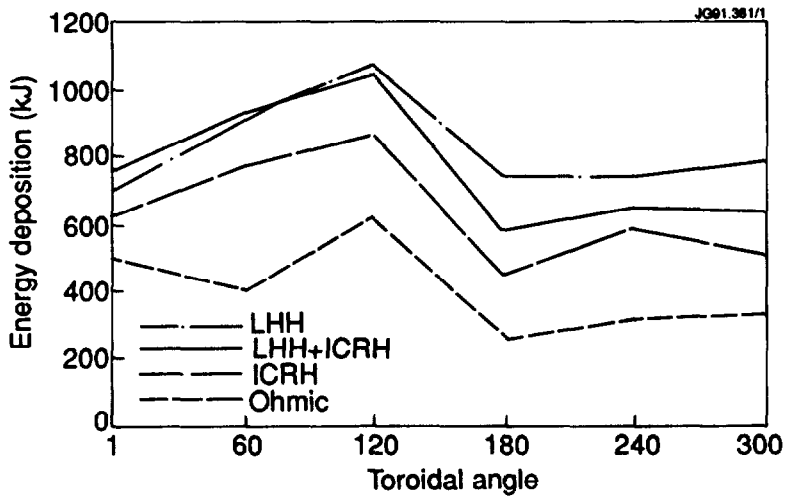

Fig. 21 Energy deposition on the inner part of the first wall for different heating methods as a function of the toroidal angle

APPENDIX 1.

THE JET TEAM

JET Joint Undertaking, Abingdon, Oxon, OX14 3EA, U.K.

J.M.Adams[1], F.Alladio[4], H.Altmann, R.J.Anderson, G.Appruzzese, W.Bailey, B.Balet, D.V.Bartlett, L.R.Baylor[24], K.Behringer, A.C.Bell, P.Bertoldi, E.Bertolini, V.Bhatnagar, R.J.Bickerton, A.Boileau[3], T.Bonicelli, S.J.Booth, G.Bosia, M.Botman, D.Boyd[31], H.Brelen, H.Brinkschulte, M.Brusati, T.Budd, M.Bures, T.Businaro[4], H.Buttgereit, D.Cacaut, C.Caldwell-Nichols, D.J.Campbell, P.Card, J.Carwardine, G.Celentano, P.Chabert[27], C.D.Challis, A.Cheetham, J.Christiansen, C.Christodoulopoulos, P.Chuilon, R.Claesen, S.Clement[30], J.P.Coad, P.Colestock[6], S.Conroy[13], M.Cooke, S.Cooper, J.G.Cordey, W.Core, S.Corti, A.E.Costley, G.Cottrell, M.Cox[7], P.Cripwell[13], F.Crisanti[4], D.Cross, H.de Blank[16], J.de Haas[16], L.de Kock, E.Deksnis, G.B.Denne, G.Deschamps, G.Devillars, K.J.Dietz, J.Dobbing, S.E.Dorling, P.G.Doyle, D.F.Düchs, H.Duquenoy, A.Edwards, J.Ehrenberg[14], T.Elevant[12], W.Engelhardt, S.K.Erents[7], L.G.Eriksonn[5], M.Evrard[2], H.Falter, D.Flory, M.Forrest[7], C.Froger, K.Fullard, M.Gadeberg[11], A.Galetsas, R.Galvao[8], A.Gibson, R.D.Gill, A.Gondhalekar, C.Gordon, G.Gorini, C.Gormezano, N.A.Gottardi, C.Gowers, B.J.Green, F.S.Griph, M.Gryzinski[26], R.Haange, G.Hammett[6], W.Han[9], C.J.Hancock, P.J.Harbour, N.C.Hawkes[7], P.Haynes[7], T.Hellsten, J.L.Hemmerich, R.Hemsworth, R.F.Herzog, K.Hirsch[14], J.Hoekzema, W.A.Houlberg[24], J.How, M.Huart, A.Hubbard, T.P.Hughes[32], M.Hugon, M.Huguet, J.Jacquinot, O.N.Jarvis, T.C.Jernigan[24], E.Joffrin, E.M.Jones, L.P.D.F.Jones, T.T.C.Jones, J.Källne, A.Kaye, B.E.Keen, M.Keilhacker, G.J.Kelly, A.Khare[15], S.Knowlton, A.Konstantellos, M.Kovanen[21], P.Kupschus, P.Lallia, J.R.Last, L.Lauro-Taroni, M.Laux[33], K.Lawson[7], E.Lazzaro, M.Lennholm, X.Litaudon, P.Lomas, M.Lorentz-Gottardi[2], C.Lowry, G.Magyar, D.Maisonnier, M.Malacarne, V.Marchese, P.Massmann, L.McCarthy[28], G.McCracken[7], P.Mendonca, P.Meriguet, P.Micozzi[4], S.F.Mills, P.Millward, S.L.Milora[24], A.Moissonnier, P.L.Mondino, D.Moreau[17], P.Morgan, H.Morsi[14], G.Murphy, M.F.Nave, M.Newman, L.Nickesson, P.Nielsen, P.Noll, W.Obert, D.O'Brien, J.O'Rourke, M.G.Pacco-Düchs, M.Pain, S.Papastergiou, D.Pasini[20], M.Paume[27], N.Peacock[7], D.Pearson[13], F.Pegoraro, M.Pick, S.Pitcher[7], J.Plancoulaine, J-P.Poffé, F.Porcelli, R.Prentice, T.Raimondi, J.Ramette[17], J.M.Rax[27], C.Raymond, P-H.Rebut, J.Removille, F.Rimini, D.Robinson[7], A.Rolfe, R.T.Ross, L.Rossi, G.Rupprecht[14], R.Rushton, P.Rutter, H.C.Sack, G.Sadler, N.Salmon[13], H.Salzmann[14], A.Santagiustina, D.Schissel[25], P.H.Schild, M.Schmid, G.Schmidt[6], R.L.Shaw, A.Sibley, R.Simonini, J.Sips[16], P.Smeulders, J.Snipes, S.Sommers, L.Sonnerup, K.Sonnenberg, M.Stamp, P.Stangeby[19], D.Start, C.A.Steed, D.Stork, P.E.Stott, T.E.Stringer, D.Stubberfield, T.Sugie[18], D.Summers, H.Summers[20], J.Taboda-Duarte[22], J.Tagle[30], H.Tamnen, A.Tanga, A.Taroni, C.Tebaldi[23], A.Tesini, P.R.Thomas, E.Thompson, K.Thomsen[11], P.Trevalion, M.Tschudin, B.Tubbing, K.Uchino[29], E.Usselmann, H.van der Beken, M.von Hellermann, T.Wade, C.Walker, B.A.Wallander, M.Walravens, K.Walter, D.Ward, M.L.Watkins, J.Wesson, D.H.Wheeler, J.Wilks, U.Willen[12], D.Wilson, T.Winkel, C.Woodward, M.Wykes, I.D.Young, L.Zannelli, M.Zarnstorff[6], D.Zasche[14], J.W.Zwart.

PERMANENT ADDRESS

1. UKAEA, Harwell, Oxon. UK.
2. EUR-EB Association, LPP-ERM/KMS, B-1040 Brussels, Belgium.
3. Institute National des Récherches Scientifique, Quebec, Canada.
4. ENEA-CENTRO Di Frascati, I-00044 Frascati, Roma, Italy.
5. Chalmers University of Technology, Göteborg, Sweden.
6. Princeton Plasma Physics Laboratory, New Jersey, USA.
7. UKAEA Culham Laboratory, Abingdon, Oxon. UK.
8. Plasma Physics Laboratory, Space Research Institute, Sao José dos Campos, Brazil.
9. Institute of Mathematics, University of Oxford, UK.
10. CRPP/EPFL, 21 Avenue des Bains, CH-1007 Lausanne, Switzerland.
11. Risø National Laboratory, DK-4000 Roskilde, Denmark.
12. Swedish Energy Research Commission, S-10072 Stockholm, Sweden.
13. Imperial College of Science and Technology, University of London, UK.
14. Max Planck Institut für Plasmaphysik, D-8046 Garching bei München, FRG.
15. Institute for Plasma Research, Gandhinagar Bhat Gujat, India.
16. FOM Instituut voor Plasmafysica, 3430 Be Nieuwegein, The Netherlands.
17. Commissiariat à L'Energie Atomique, F-92260 Fontenay-aux-Roses, France.
18. JAERI, Tokai Research Establishment, Tokai-Mura, Naka-Gun, Japan.
19. Institute for Aerospace Studies, University of Toronto, Downsview, Ontario, Canada.
20. University of Strathclyde, Glasgow, G4 ONG, U.K.
21. Nuclear Engineering Laboratory, Lapeenranta University, Finland.
22. JNICT, Lisboa, Portugal.
23. Department of Mathematics, Univeristy of Bologna, Italy.
24. Oak Ridge National Laboratory, Oak Ridge, Tenn., USA.
25. G.A. Technologies, San Diego, California, USA.
26. Institute for Nuclear Studies, Swierk, Poland.
27. Commissiariat à l'Energie Atomique, Cadarache, France.
28. School of Physical Sciences, Flinders University of South Australia, South Australia SO42.
29. Kyushi University, Kasagu Fukuoka, Japan.
30. Centro de Investigaciones Energeticas Medioambientales y Techalogicas, Spain.
31. University of Maryland, College Park, Maryland, USA.
32. University of Essex, Colchester, UK.
33. Akademie de Wissenschaften, Berlin, DDR.

CR 88.49.1A